Kinetic Modeling of Free-Radical Graft Polymerization

Mark Chaimberg and Yoram Cohen
Dept. of Chemical Engineering, University of California, Los Angeles, CA 90024

The kinetic model of free-radical surface graft polymerization developed is based on a conservational polymerization and molecular-weight distribution (CPMWD) numerical algorithm. The CPMWD model uses an implicit numerical technique to solve for the coupled monomer, surface site, and total growing polymer differential rate equations, which ensure that conservation of mass is maintained. The model formulation allows for the incorporation of kinetic rate coefficients, which are a function of the chain length of the reacting species, the solution viscosity, and the concentration of surface grafted polymer. The model also makes it possible to evaluate the monomer conversion, the graft yield and the molecular weight distributions of the homopolymer and surface-grafted polymer for the complete duration of the graft polymerization reaction. Its application was demonstrated for a model system of vinylpyrrolidone graft polymerization onto the surface of a silica substrate.

Introduction

Graft polymerization is characterized by the growth of polymer chains from the surface of a substrate. The chemically grafted polymer layer modifies the surface chemistry of the substrate while the basic geometry of the solid substrate remains intact. As a result, the interfacial properties of the substrate can be altered to control the interactions between the substrate surface and the bulk fluid or solutes (Browne et al., 1991; Chaimberg and Cohen, 1991; Heffernan and Sherrington, 1984; Krasilnikov and Borisova, 1988; Parnas et al., 1989; Wheals, 1975).

The technique of graft polymerization has been investigated for a wide range of solid substrates, including inorganic oxides, carbon black and polymer films and fibers. The unique requirement for the solid substrate is the presence of surface reactive sites from which polymer chains can propagate. For free-radical graft polymerization reactions, the substrate is often modified to produce surface-bonded carbonyl reactive groups (Browne et al., 1992; Chaimberg et al., 1989; Chaimberg and Cohen, 1991; Korshak et al., 1979; Krasilnikov and Borisova, 1988; Laible and Hamann, 1980; Monrabal, 1981; Wheals, 1975; Zubakova et al., 1987) or surface-bonded initiators (Laible and Hamann, 1980; Yablokova et al., 1986).

Correspondence concerning this article should be addressed to Y. Cohen.
Current address of M. Chaimberg: Swing Paints Limited, 2100 St. Patrick St., Montreal, Quebec H3K-1B1, Canada.

Free-radical graft polymerization reaction involves the consumption of monomer units in producing growing polymer chains from surface reactive sites (Figure 1). During the reaction, however, monomer units may also form homopolymer chains. Live homopolymer chains can chemically bond to the support surface directly via polymer grafting, resulting in additional increase of the amount of grafted polymer. Since polymer molecules must diffuse to the solid surface, diffusional limitations and steric hindrance effects severely reduce the number of surface-bonded polymer chains obtained by this polymer grafting reaction (Papirer and Nguyen, 1973) and thus the uniformity of the polymer layer. In contrast, in the graft polymerization reaction, the smaller monomers diffuse to the surface with significantly less steric hindrance effects relative to graft polymerization. It is interesting to note that in some size exclusion chromatography applications, a stable and uniform polymer surface layer, especially within the porous matrix of the silica resin, is required to prevent the nonspecific interactions of solutes with the silica (Cohen and Eisenberg, 1992; Cohen et al., 1992; Parnas et al., 1989). To achieve the desired characteristics for the grafted material, it is necessary to comprehensively understand the specific reactions involved in graft polymerization.

Considerable work has been done to ascertain the effect of various reaction conditions on graft polymerization (for ex-

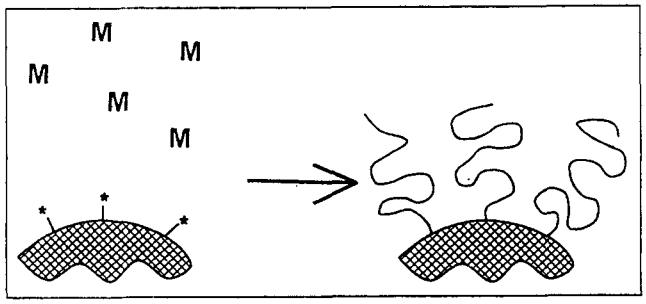

Figure 1. Graft polymerization reaction system.

ample, monomer concentration and reaction temperature). Kinetic models which have been proposed to describe the mechanism of graft polymerization are restricted to special cases (Fox et al., 1959; Nayak et al., 1978; Sahoo et al., 1986; S. Samal et al., 1984; R. Samal et al., 1984; Sundardi, 1978; Tripathy et al., 1985; Hernandez, 1990). Qualitative analytical solutions yielding the order of the grafting reaction (Fox et al., 1959; Nayak et al., 1978; S. Samal et al., 1984; Sundardi, 1978; Tripathy et al., 1985) and the number-average molecular weight of the grafted polymer (Fox et al., 1959) were obtained by employing a variety of assumptions, including the quasi-steady-state assumption (QSSA) and the long-chain hypothesis (LCH). The use of the QSSA and LCH in numerical algorithms, however, is limited. The LCH is a valid approximation when the polymerization reaction results in a large kinetic chain length and may be invalid if the ratio of monomer-to-initiator consumption rates is relatively high, as in the case for very fast initiation *reactions* (Biesenberger and Sebastian, 1983). The QSSA is not applicable for systems in which there is a rapid rate of initiator decomposition, as in dead-end polymerization (Biesenberger and Sebastian, 1983), or for cases where hindered radical termination results in a gel effect (Biesenberger and Sebastian, 1983; Chiu et al., 1983; Ito, 1969). Furthermore, application of the QSSA violates the mass-balance constraint for the system of equations and can result in errors in the calculation of the individual species' concentrations (Chaimberg and Cohen, 1990). In numerical simulations, the propagation of the error in the individual species concentrations may become significant, thereby resulting in large errors in the overall mass balance (Edelson, 1973; Gelinas, 1972). Existing graft polymerization kinetic models do not determine the overall mass balance accurately. This is *essential* for graft polymerization reactions which result in the formation of both homopolymer and grafted polymer species, especially when low yields or *short chains* of the grafted polymer are obtained (Chaimberg et al., 1989; Chaimberg and Cohen, 1991; Domb and Avny, 1984; Raval et al., 1988; Vasantha et al., 1987). It is important to note that the available kinetic models for graft polymerization are *incapable* of predicting the amount of polymer grafted onto the substrate (graft yield) and the polymer molecular-weight distribution (MWD) as a function of reaction time. Moreover, existing graft polymerization models have not considered the effect of chain-length and graft density on the reaction rate parameters.

This work describes a detailed analysis method for the free-radical graft polymerization reaction. The kinetic scheme for the reaction system is presented, followed by the details of the system of rate equations, and the conservational polymerization and molecular-weight distribution (CPMWD) numerical algorithm (Chaimberg and Cohen, 1990) used to solve the model equations. The CPMWD algorithm is founded on the requirement of maintaining a strict mass balance for all species, allowing for the accurate determination of the graft yield and the complete MWD of the polymer. Previous work by Chaimberg and Cohen (1990) demonstrated the ability of the CPMWD approach to incorporate complex phenomena, such as the onset of gelation and chain-length-dependent kinetic rate coefficients.

In this work, the CPMWD model was applied to the aqueous-phase free-radical graft polymerization of vinylpyrrolidone (VP) onto vinylsilane-modified silica particles to form polyvinylpyrrolidone (PVP)-graft silica. Detailed experimental data for the PVP-graft-silica system were recently published by Chaimberg et al. (1989) and Chaimberg and Cohen (1991). It is interesting to note that PVP is a nontoxic and biocompatible polymer which is soluble in aqueous as well as many organic solvents. Recently, PVP-graft-silica has shown promise as an adsorbent for the removal of chlorinated hydrocarbons from aqueous solutions (Browne et al., 1992), a chromatographic support resin useful in preventing nonspecific adsorption of solutes in aqueous phase-size exclusion chromatography (Cohen and Eisenberg, 1992; Cohen et al., 1992), and as a resin for the chromatographic separation of viruses (Krasilnikov and Borisova, 1988).

Theory

The graft polymerization kinetic model presented in this work accounts for the reactions of the following species: solvent, monomer in solution, surface-bound monomer, initiator, free radical, free-radical growing homopolymer chains, free-radical growing surface chains, and terminated ("dead") homopolymer and terminally anchored surface chains. The graft polymerization kinetic model was solved using the CPMWD algorithm. The CPMWD algorithm is based on the use of an implicit numerical technique to solve for the coupled monomer, surface site, total growing homopolymer and total graft polymer concentration differential equations. Acceleration of the numerical calculations is achieved by lumping the growing homopolymer and graft polymer chains into distinct groups. The proposed numerical scheme generates the monomer conversion, the graft yield, and a complete molecular-weight distribution of the growing and dead homopolymer and graft polymer species. The current formulation allows for the incorporation of nonidealities, such as the graft-yield- and chain-length-dependent kinetic rate coefficients.

Graft polymerization kinetic model

The overall reaction scheme for free-radical graft polymerization can be represented by the following reaction steps, in which the reaction rate coefficients are chain-length-dependent.

Initiation:

$$I \xrightarrow{k_d} 2R. \tag{1}$$

$$R\cdot + M \xrightarrow{k_{iM}} M_1. \tag{2}$$

$$R\cdot + S \xrightarrow{k_{iS}} S_1. \tag{3}$$

Homopolymer Propagation (in Solution):

$$\begin{aligned} M\cdot_1 + M &\xrightarrow{k_{pMM(1)}} M\cdot_2 \\ &\vdots \quad \vdots \quad \vdots \\ M\cdot_n + M &\xrightarrow{k_{pMM(n)}} M\cdot_{n+1} \end{aligned} \tag{4}$$

Polymer Grafting onto Surface Sites:

$$\begin{aligned} M\cdot_1 + S &\xrightarrow{k_{pMS(1)}} S\cdot_2 \\ &\vdots \quad \vdots \quad \vdots \\ M\cdot_n + S &\xrightarrow{k_{pMS(n)}} S\cdot_{n+1} \end{aligned} \tag{5}$$

Graft Polymer Propagation on Surface Sites:

$$\begin{aligned} S\cdot_1 + M &\xrightarrow{k_{pSM(1)}} S\cdot_2 \\ &\vdots \quad \vdots \quad \vdots \\ S\cdot_n + M &\xrightarrow{k_{pSM(n)}} S\cdot_{n+1} \end{aligned} \tag{6}$$

Chain Transfer:

$$M\cdot_n + M \xrightarrow{k_{trMM(n)}} H_n + M\cdot_1 \tag{7}$$

$$M\cdot_n + S \xrightarrow{k_{trMS(n)}} H_n + S\cdot_1 \tag{8}$$

$$M\cdot_n + X \xrightarrow{k_{trMX(n)}} H_n + M\cdot_1 \tag{9}$$

$$S\cdot_n + M \xrightarrow{k_{trSM(n)}} G_n + M\cdot_1 \tag{10}$$

$$S\cdot_n + S \xrightarrow{k_{trSS(n)}} G_n + S\cdot_1 \tag{11}$$

$$S\cdot_n + X \xrightarrow{k_{trSX(n)}} G_n + M\cdot_1 \tag{12}$$

Termination:

$$M\cdot_m + M\cdot_n \xrightarrow{k_{tcMM(m,n)}} H_{m+n} \tag{13}$$

$$M\cdot_m + M\cdot_n \xrightarrow{k_{tdMM(m,n)}} H_m + H_n \tag{14}$$

$$M\cdot_m + S\cdot_n \xrightarrow{k_{tcMS(m,n)}} G_{m+n} \tag{15}$$

$$M\cdot_m + S\cdot_n \xrightarrow{k_{tdMS(m,n)}} H_m + G_n \tag{16}$$

$$S\cdot_m + S\cdot_n \xrightarrow{k_{tcSS(m,n)}} G_{m+n} \tag{17}$$

$$S\cdot_m + S\cdot_n \xrightarrow{k_{tdSS(m,n)}} G_m + G_n \tag{18}$$

where I is the initiator, $R\cdot$ is an initiator radical, M is the monomer, S is the surface site, $M\cdot_n$ is a growing homopolymer chain of length n, $S\cdot_n$ is a growing grafted polymer chain of length n, H_n is a dead homopolymer chain of length n, G_n is a dead grafted polymer chain of length n and X is the solvent. The reaction rate coefficient for homopolymer propagation of a growing homopolymer with chain length n, is given by $k_{pMM(n)}$ (Eq. 4). The polymer grafting reaction rate coefficient, $k_{pMS(n)}$, is for the reaction of a growing homopolymer species of chain length n with a surface site to produce a growing grafted polymer chain (Eq. 5). The graft polymer propagation reaction rate coefficient, $k_{pSM(n)}$, is for the reaction of a growing grafted polymer with chain length n with a monomer (Eq. 6). The reaction rate coefficients for chain transfer of a growing homopolymer species of chain length n with a monomer, surface site and solvent are given by $k_{trMM(n)}$, $k_{trMS(n)}$ and $k_{trMX(n)}$, respectively (Eqs. 7-9). Similarly, the reaction rate coefficients for chain transfer of a growing grafted polymer species of chain length n with a monomer, surface site and solvent are given by $k_{trSM(n)}$, $k_{trSS(n)}$ and $k_{trSX(n)}$, respectively (Eqs. 10-12). The combination and disproportionation termination reaction rate coefficients are given by: $k_{tcMM(m,n)}$ and $k_{tdMM(m,n)}$ for the termination of two growing homopolymers with chain lengths m and n (Eqs. 13 and 14), $k_{tcSM(m,n)}$ and $k_{tdSM(m,n)}$ for the termination of a growing homopolymer species of chain length m with a growing grafted polymer of chain length n (Eqs. 15 and 16), and $k_{tcSS(m,n)}$ and $k_{tdSS(m,n)}$ for the termination of two growing grafted polymers with chain lengths m and n (Eqs. 17 and 18). Finally, the initiation scheme, defined by Eqs. 1-3, is for decomposition of the usual type of chemical initiators (for example, peroxide and diazo compounds). It is noted that the hydrogen peroxide initiator, used by Chaimberg and Cohen (1991) for vinylpyrrolidone graft polymerization, will decompose into two initiator free radicals (Evans and Upton, 1985). Other mechanisms of initiation, such as thermal or biomolecular initiation, or *initiations that can be described by the Cage-Effect, Complex Theory or hybrid initiation models* (Hunkeler, 1991) can be readily incorporated into the reaction scheme without a loss of generality in the general modeling approach that is discussed below.

The kinetic rate expressions for various species resulting from the above system of equations (Eqs. 1-18) are:

For the Initiator:

$$\frac{1}{V}\frac{d(IV)}{dt} = -k_d I \tag{19}$$

$$\frac{1}{V}\frac{d(R\cdot V)}{dt} = 2(f_M + f_S)k_d I - k_{iM} M R\cdot - k_{iS} S R \tag{20}$$

where f_M and f_S are the initiator efficiencies (note that $f_M + f_S \leq 1$) for M and S, respectively, and V is the volume of the reaction mixture.

For the Growing Homopolymer Species:

$$\begin{aligned} \frac{1}{V}\frac{d(M\cdot_1 V)}{dt} &= k_{iM} M R\cdot - k_{pMM(1)} M M\cdot_1 - (k_{pMS(1)} + k_{trMS(1)}) S M\cdot_1 \\ &+ \sum_{i=2}^{\infty} (k_{trMM(i)} M + k_{trMX(i)} X) M\cdot_i + \sum_{i=1}^{\infty} (k_{trSM(i)} M + k_{trSX(i)} X) S\cdot_i \\ &- M\cdot_i \sum_{i=1}^{\infty} [(k_{tcMM(1,i)} + k_{tdMM(1,i)}) M\cdot_i \\ &+ (k_{tcMS(1,i)} + k_{tdMS(1,i)}) S\cdot_i] \end{aligned} \tag{21}$$

$$\frac{1}{V}\frac{d(M\cdot_n V)}{dt} = (k_{pMM(n-1)}M\cdot_{n-1} - k_{pMM(n)}M\cdot_n)M - [k_{trMM(n)}M + (k_{pMS(n)} + k_{trMS(n)})S + k_{trMX(n)}X]M\cdot_n - M\cdot_n\sum_{i=1}^{\infty}[(k_{tcMM(n,i)} + k_{tdMM(n,i)})M\cdot_i + (k_{tcMS(n,i)} + k_{tdMS(n,i)})S\cdot_i] \qquad n \geq 2 \quad (22)$$

$$\frac{1}{V}\frac{d(M\cdot V)}{dt} = k_{iM}MR\cdot + \sum_{i=1}^{\infty}(k_{trSM(i)}M + k_{trSX(i)}X)S\cdot_i - S\sum_{i=1}^{\infty}(k_{pMS(i)} + k_{trMS(i)})M\cdot_i - \sum_{i=1}^{\infty}\sum_{j=1}^{\infty}(k_{tcMM(i,j)} + k_{tdMM(i,j)})M\cdot_i M\cdot_j - \sum_{i=1}^{\infty}\sum_{j=1}^{\infty}(k_{tcMS(i,j)} + k_{tdMS(i,j)})M\cdot_i S\cdot_j \quad (23)$$

where $M\cdot$ is the total concentration of growing homopolymer chains, given by:

$$M\cdot = \sum_{i=1}^{\infty}M\cdot_i \quad (24)$$

For the Growing Grafted Polymer Species:

$$\frac{1}{V}\frac{d(S\cdot_1 V)}{dt} = k_{iS}SR\cdot - (k_{pSM(1)} + k_{trSM(1)})MS\cdot_1 - k_{trSX(1)}XS\cdot_1 + S\sum_{i=1}^{\infty}k_{trMS(i)}M\cdot_i + S\sum_{i=2}^{\infty}k_{trSS(i)}S\cdot_i - S\cdot_1\sum_{i=1}^{\infty}[(k_{tcMS(1,i)} + k_{tdMS(1,i)}]M\cdot_i + (k_{tcSS(1,i)} + k_{tdSS(1,i)})S\cdot_i] \quad (25)$$

$$\frac{1}{V}\frac{d(S\cdot_n V)}{dt} = (k_{pSM(n-1)}S\cdot_{n-1} - k_{pSM(n)}S\cdot_n)M + k_{pMS(n-1)}SM\cdot_{n-1} - (k_{trSM(n)}M + k_{trSS(n)}S + k_{trSX(n)}X)S\cdot_n - S\cdot_n\sum_{i=1}^{\infty}[(k_{tcMS(n,i)} + k_{tdMS(n,i)})M\cdot_i + (k_{tcSS(n,i)} + k_{tdSS(n,i)})S\cdot_i] \qquad n \geq 2 \quad (26)$$

$$\frac{1}{V}\frac{d(S\cdot V)}{dt} = k_{iS}SR\cdot + S\sum_{i=1}^{\infty}(k_{pMS(i)} + k_{trMS(i)})M\cdot_i - \sum_{i=1}^{\infty}(k_{trSM(i)}M + k_{trSX(i)}X)S\cdot_i - \sum_{i=1}^{\infty}\sum_{j=1}^{\infty}(k_{tcMS(i,j)} + k_{tdMS(i,j)})M\cdot_i S\cdot_j - \sum_{i=1}^{\infty}\sum_{j=1}^{\infty}(k_{tcSS(i,j)} + k_{tdSS(i,j)})S\cdot_i S\cdot_j \quad (27)$$

where $S\cdot$ is the total concentration of growing graft polymer chains given by:

$$S\cdot = \sum_{i=1}^{\infty}S\cdot_i \quad (28)$$

For the Monomer, Surface Sites, Dead Homopolymer, and Dead Grafted Polymer Species:

$$\frac{1}{V}\frac{d(MV)}{dt} = -k_{iM}MR\cdot + (k_{trMM(1)}M + k_{trMS(1)}S + k_{trMX(1)}X)M\cdot_1 - M\sum_{i=1}^{\infty}(k_{pMM(i)} + k_{trMM(i)})M\cdot_i - M\sum_{i=1}^{\infty}(k_{pSM(i)} + k_{trSM(i)})S\cdot_i + M\cdot_1\sum_{i=1}^{\infty}(k_{tdMM(1,i)}M\cdot_i + k_{tdMS(1,i)}S\cdot_i) \quad (29)$$

$$\frac{1}{V}\frac{d(H_n V)}{dt} = (k_{trMM(n)}M + k_{trMS(n)}S + k_{trMX(n)}X)M\cdot_n + \frac{1}{2}\sum_{i=1}^{\infty}k_{tcMM(i,n-i)}M\cdot_i M\cdot_{n-i} + M\cdot_n\sum_{i=1}^{\infty}(k_{tdMM(n,i)}M\cdot_i + k_{tdMS(n,i)}S\cdot_i), \quad n \geq 2 \quad (30)$$

$$\frac{1}{V}\frac{d(SV)}{dt} = -k_{iS}SR\cdot + (k_{trSM(1)}M + k_{trSS(1)}S + k_{trSX(1)}X)S\cdot_1 - S\sum_{i=1}^{\infty}(k_{pMS(i)} + k_{trMS(i)})M\cdot_i - S\sum_{i=1}^{\infty}k_{trSS(i)}S\cdot_i + S\cdot_1\sum_{i=1}^{\infty}(k_{tdMS(1,i)}M\cdot_i + k_{tdSS(1,i)}S\cdot_i) \quad (31)$$

$$\frac{1}{V}\frac{d(G_n V)}{dt} = (k_{trSM(n)}M + k_{trSS(n)}S + k_{trSX(n)}X)S\cdot_n + \frac{1}{2}\sum_{i=1}^{\infty}(k_{tcMS(i,n-i)}M\cdot_i + k_{tcSS(i,n-i)}S\cdot_i)S\cdot_{n-i} + S\cdot_n\sum_{i=1}^{\infty}(k_{tdMS(n,i)}M\cdot_i + k_{tdSS(n,i)}S\cdot_i), \quad n \geq 2 \quad (32)$$

The reaction volume, V, is related to the volume concentration, ϵ, the monomer conversion, x, and the initial volume fraction of monomer, ϕ_{M_o}:

$$V = V_o(1 - \epsilon x\phi_{M_o}) \quad (33)$$

$$\epsilon = \frac{\rho_H - \rho_M}{\rho_H} \quad (34)$$

$$x = \frac{M_o V_o - MV}{M_o V_o} \quad (35)$$

where V_o is the initial volume of the reaction mixture, M_o is the initial monomer concentration, and ρ_H and ρ_M are the

densities of the pure homopolymer and pure monomer, respectively.

CPMWD algorithm

The variation of the initiator concentration with time can be determined analytically from Eq. 19 and yields:

$$IV = I_o V_o e^{-k_d t} \tag{36}$$

It is generally accepted that the QSSA can be applied to the initiator radicals, $R\cdot$, formed by the decomposition of the type of chemical initiator considered in the current study (Eq. 1). The use of this approximation in Eq. 20 leads to:

$$2(f_M + f_S)k_d I = k_{iM} M R\cdot + k_{iS} S R\cdot \tag{37}$$

Furthermore, since the initiation of monomer and surface sites are independent of each other, one may distinguish between the two types of initiations and obtain:

$$2f_M k_d I = k_{iM} M R\cdot \tag{38}$$

$$2f_S k_d I = k_{iS} S R\cdot \tag{39}$$

In the present approach, to formulate a finite system of differential equations for the time rate of change of the species concentrations which can be solved numerically, a maximum growing polymer chain length above which no propagation to higher chain length growing polymers occurs is set. The maximum chain length must be reset if the determined MWD indicates that the concentration of largest chain polymer is non-negligible. The restriction on the maximum growing polymer chain length, N, sets an upper limit on the chain size of the dead polymer to be $2N$, due to the possibility of combination of the largest growing polymer chains (Eqs. 13, 15 and 17). Thus, the *solution* of the set of stiff differential Eqs. 21–32 requires the numerical integration of $6N$ equations. However, it is not necessary to solve $6N$ differential equations since the total mass balance is maintained by solving Eqs. 23 and 27 and 29–32, which form a consistent set of mass balance equations. In the CPMWD algorithm, implicit trapezoidal integration (Gear, 1971) is used to solve Eqs. 23 and 27 for the total growing homopolymer and graft polymer concentrations, respectively, coupled with the time rate of change of the monomer and surface site concentrations (Eqs. 29 and 31). The implicit method has the advantage of permitting the use of relatively large time steps while maintaining numerical stability. Once the total growing homopolymer and graft polymer concentrations are known, the QSSA may be applied to Eqs. 21, 22, 25 and 26 to determine the individual growing polymer concentrations.

The numerical calculations involved in solving for the growing polymer concentrations, although simplified by the application of the QSSA, are still extensive due to the $2N$ coupled algebraic equations that must be solved. In order to make the numerical solution more tractable, the growing homopolymer and graft polymer chains are lumped into ν distinct groups. The group concentration is denoted by $\mu\cdot_i$ and $\sigma\cdot_i$ for the growing homopolymer and graft polymer chains, respectively, where the number of growing polymer chains lumped into group i is given by λ_i (Skeirik and Grulke, 1985). For example, the group concentration of a series of growing homopolymer and graft polymer species with chain lengths from a_1 to a_n is given by:

$$\mu\cdot_i = \sum_{j=a_1}^{a_n} M\cdot_j \tag{40}$$

$$\sigma\cdot_i = \sum_{j=a_1}^{a_n} S\cdot_j \tag{41}$$

and the number of growing polymer chains lumped into group i, λ_i, is defined as:

$$\lambda_i = a_n - a_1 + 1 \tag{42}$$

The lumping of the growing polymer chains into ν number of groups results in the following rate equations for the groups of growing polymer chains:

$$\frac{1}{V}\frac{d(\mu\cdot_1 V)}{dt} = 2f_M k_d I - \kappa_{pMM(1)} M \frac{\mu\cdot_1}{\lambda_1} - (\kappa_{pMS(1)} + \kappa_{trMS(1)}) S \mu\cdot_1 + \sum_{i=2}^{\nu} (\kappa_{trMM(i)} M + \kappa_{trMX(i)} X)\mu\cdot_i + \sum_{i=1}^{\nu} (\kappa_{trSM(i)} M + \kappa_{trSX(i)} X)\sigma\cdot_i - \mu\cdot_1 \sum_{i=1}^{\nu} [\delta_{1,i}(\kappa_{tcMM(1,i)} + \kappa_{tdMM(1,i)})\mu\cdot_i + (\kappa_{tcMS(1,i)} + \kappa_{tdMS(1,i)})\sigma\cdot_i] \tag{43}$$

$$\frac{1}{V}\frac{d(\mu\cdot_n V)}{dt} = \left(\kappa_{pMM(n-1)}\frac{\mu\cdot_{n-1}}{\lambda_{n-1}} - \kappa_{pMM(n)}\frac{\mu\cdot_n}{\lambda_n}\right) M - [\kappa_{trMM(n)} M + (\kappa_{pMS(n)} + \kappa_{trMS(n)}) S + \kappa_{trMX(n)} X]\mu\cdot_n - \mu\cdot_n \sum_{i=1}^{\nu} [\delta_{n,i}(\kappa_{tcMM(n,i)} + \kappa_{tdMM(n,i)})\mu\cdot_i + (\kappa_{tcMS(n,i)} + \kappa_{tdMS(n,i)})\sigma\cdot_i] \qquad 2 \le n \le \nu - 1 \tag{44}$$

$$\frac{1}{V}\frac{d(\mu\cdot_\nu V)}{dt} = \kappa_{pMM(\nu-1)}\frac{\mu\cdot_{\nu-1}}{\lambda_{\nu-1}} M - (\kappa_{trMM(\nu)} M + \kappa_{trMS(\nu)} S + \kappa_{trMX(\nu)} X)\mu\cdot_\nu - \mu\cdot_\nu \sum_{i=1}^{\nu} [\delta_{\nu,i}(\kappa_{tcMM(\nu,i)} + \kappa_{tdMM(\nu,i)})\mu\cdot_i + (\kappa_{tcMS(\nu,i)} + \kappa_{tdMS(\nu,i)})\sigma\cdot_i] \tag{45}$$

$$\frac{1}{V}\frac{d(\sigma\cdot_1 V)}{dt} = 2f_S k_d I - \kappa_{pSM(1)} M \frac{\sigma\cdot_1}{\lambda_1} - \kappa_{pMS(1)} S \mu\cdot_1 \frac{\lambda_1 - 1}{\lambda_1} - (\kappa_{trSM(1)} M + \kappa_{trSX(1)} X)\sigma\cdot_1 + S\sum_{i=1}^{\nu} \kappa_{trMS(i)}\mu\cdot_i + S\sum_{i=2}^{\nu} \kappa_{trSS(i)}\sigma\cdot_i - \sigma\cdot_1 \sum_{i=1}^{\nu} [(\kappa_{tcMS(1,i)} + \kappa_{tdMS(1,i)})\mu\cdot_i + \delta_{1,i}(\kappa_{tcSS(1,i)} + \kappa_{tdSS(1,i)})\sigma\cdot_i] \tag{46}$$

$$\frac{1}{V}\frac{d(\sigma^{\cdot}_{n}V)}{dt}=\left(\kappa_{pSM(n-1)}\frac{\sigma^{\cdot}_{n-1}}{\lambda_{n-1}}-\kappa_{pSM(n)}\frac{\sigma^{\cdot}_{n}}{\lambda_{n}}\right)M+\left(\kappa_{pMS(n-1)}\frac{\mu^{\cdot}_{n-1}}{\lambda_{n-1}}-\kappa_{pMS(n)}\mu^{\cdot}_{n}\frac{\lambda_{n}-1}{\lambda_{n}}\right)S-(\kappa_{trSM(n)}M+\kappa_{trSS(n)}S+\kappa_{trSX(n)}X)\sigma^{\cdot}_{n}-\sigma^{\cdot}_{n}\sum_{i=1}^{\nu}[(\kappa_{tcMS(n,i)}+\kappa_{tdMS(n,i)})\mu^{\cdot}_{i}+\delta_{n,i}(\kappa_{tcSS(n,i)}+\kappa_{tdSS(n,i)})\sigma^{\cdot}_{i}]$$

$$2\le n\le \nu-1 \quad (47)$$

$$\frac{1}{V}\frac{d(\sigma^{\cdot}_{\nu}V)}{dt}=\kappa_{pSM(\nu-1)}M\frac{\sigma^{\cdot}_{\nu-1}}{\lambda_{\nu-1}}+\left(\kappa_{pMS(\nu-1)}\frac{\mu^{\cdot}_{\nu-1}}{\lambda_{\nu-1}}-\kappa_{pMS(\nu)}\mu^{\cdot}_{\nu}\frac{\lambda_{\nu}-1}{\lambda_{\nu}}\right)S-(\kappa_{trSM(\nu)}M+\kappa_{trSS(\nu)}S+\kappa_{trSX(\nu)}X)\sigma^{\cdot}_{\nu}-\sigma^{\cdot}_{\nu}\sum_{i=1}^{\nu}[(\kappa_{tcMS(\nu,i)}+\kappa_{tdMS(\nu,i)})\mu^{\cdot}_{i}+\delta_{\nu,i}(\kappa_{tcSS(\nu,i)}+\kappa_{tdSS(\nu,i)})\sigma^{\cdot}_{i}] \quad (48)$$

where

$$\delta_{i,j}=\begin{cases}1, & i\neq j\\ 2, & i=j\end{cases}$$

$\kappa_{pMM(n)}$, $\kappa_{pMS(n)}$ and $\kappa_{pSM(n)}$ are the group reaction rate coefficients for the growing polymer group number n undergoing homopolymer propagation, polymer grafting, and graft polymer propagation, respectively. The group reaction rate coefficients for chain transfer with monomer, surface sites, and solvent are given by $\kappa_{trMM(n)}$, $\kappa_{trMS(n)}$, and $\kappa_{trMX(n)}$ for chain transfer reactions with the growing homopolymer group number m, and by $\kappa_{trSM(n)}$, $\kappa_{trSS(n)}$, and $\kappa_{trSX(n)}$ for chain transfer reactions with the growing graft polymer group number n. The combination and disproportionation termination group reaction rate coefficients $\kappa_{tcMM(m,n)}$ and $\kappa_{tdMM(m,n)}$, $\kappa_{tcMS(m,n)}$ and $\kappa_{tdMS(m,n)}$, and $\kappa_{tcss(m,n)}$ and $\kappa_{tdss(m,n)}$, are for the termination reactions of the growing homopolymer group numbers m and n, growing homopolymer group number m and growing graft polymer group number n, and growing graft polymer group numbers m and n, respectively.

Application of the QSSA to the groups of growing polymers defined in Eqs. 43–48 transforms the set of differential equations into a set of algebraic equations which are used to obtain the concentrations of the groups of growing polymers. The concentrations of the individual growing polymer chains, $M^{\cdot}_{i}$ and $S^{\cdot}_{i}$, are determined from a cubic spline interpolation technique. The nodes of the cubic spline are defined at the average chain length of each group j to have a corresponding average lumped group concentration of $(\mu^{\cdot}_{j}/\lambda_{j})$ for the growing homopolymer and $(\sigma^{\cdot}_{j}/\lambda_{j})$ for the growing graft polymer species.

Finally, the rate of homopolymer (Eq. 30) and grafted polymer (Eq. 32) formation can be rewritten to incorporate the maximum chain length, N, and the group lumping of the growing polymer species as:

$$\frac{1}{V}\frac{d(H_{n}V)}{dt}=(k_{trMM(n)}M+k_{trMS(n)}S+k_{trMX(n)}X)M^{\cdot}_{n}+\frac{1}{2}\sum_{i=1}^{N}k_{tcMM(i,n-i)}M^{\cdot}_{i}M^{\cdot}_{n-i}+M^{\cdot}_{n}\sum_{i=1}^{\nu}(\kappa_{tdMM(n,i)}\mu^{\cdot}_{i}+\kappa_{tdMS(n,i)}\sigma^{\cdot}_{i}),\quad n\le N \quad (49)$$

$$\frac{1}{V}\frac{d(H_{n}V)}{dt}=\frac{1}{2}\sum_{i=n-N}^{N}k_{tcMM(i,n-i)}M^{\cdot}_{i}M^{\cdot}_{n-i},\quad N<n\le 2N \quad (50)$$

$$\frac{1}{V}\frac{d(G_{n}V)}{dt}=(k_{trSM(n)}M+k_{trSS(n)}S+k_{trSX(n)}X)S^{\cdot}_{n}+\frac{1}{2}\sum_{i=1}^{N}(k_{tcMS(i,n-i)}M^{\cdot}_{i}+k_{tcSS(i,n-i)}S^{\cdot}_{i})S^{\cdot}_{n-i}+S^{\cdot}_{n}\sum_{i=1}^{\nu}(\kappa_{tdMS(n,i)}\mu^{\cdot}_{i}+\kappa_{tdSS(n,i)}\sigma^{\cdot}_{i}),\quad n\le N \quad (51)$$

$$\frac{1}{V}\frac{d(G_{n}V)}{dt}=\frac{1}{2}\sum_{i=n-N}^{N}(k_{tcMS(i,n-i)}M^{\cdot}_{i}+k_{tcSS(i,n-i)}S^{\cdot}_{i})S^{\cdot}_{n-i},\quad N<n\le 2N \quad (52)$$

In general, the MWD of the dead polymer species is assumed to be a continuous distribution. As a result, one need only solve Eqs. 49–52 for a discrete number of chain lengths, which

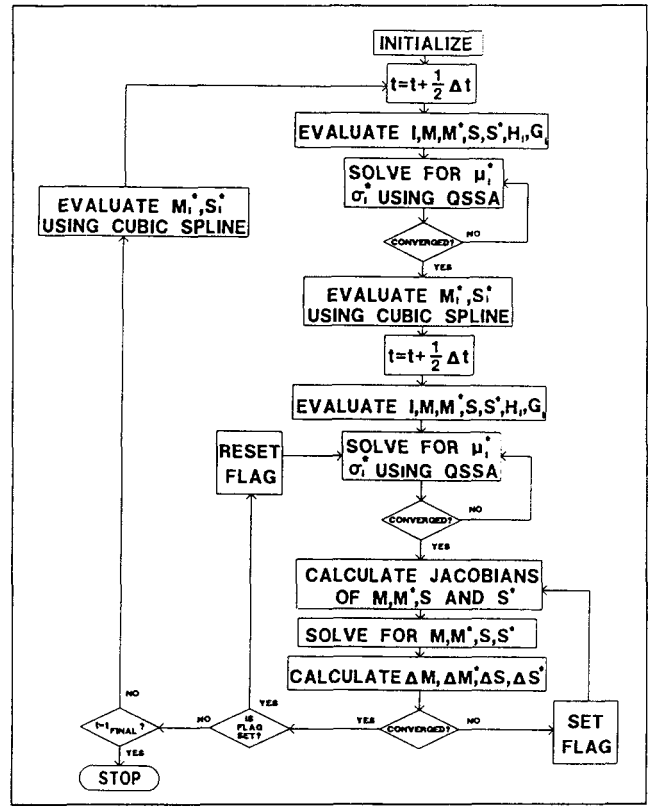

Figure 2. Flowsheet of CPMWD numerical simulation.

are then used as the nodes for the cubic spline interpolation technique to solve for the concentrations of the remaining dead polymer chains.

The numerical scheme used to solve the free-radical graft polymerization reaction system (Eqs. 23, 27, 29, 31, 36 and 43-52) is shown schematically in Figure 2. At each time step, the initiator concentration is evaluated directly from Eq. 36. A Newton-Raphson iteration technique is then used to solve the coupled implicit equations associated with trapezoidal integration of Eqs. 23, 27, 29 and 31. The simultaneous solution for the monomer, surface site and total combined growing polymer concentrations guarantees that conservation of mass is maintained for every species in the system. Subsequently, the QSSA is applied to Eqs. 43-48 and the lumped growing polymer concentrations are determined by an iterative numerical technique. The individual growing polymer species concentrations are calculated by a cubic spline interpolation algorithm with nodes corresponding to the average concentration of the group of growing polymer chains at the average chain length of the group. The dead polymer species concentrations are determined by integration of Eqs. 49-52.

The accuracy of the numerical method and the determination of the optimal growing parameters were evaluated by the following three criteria: conservation of mass, growing polymer concentration, and concentration of the maximum chain length group. The conservation of mass criterion was determined by a comparison of the initial mass of the system with the total mass of the system at each time step as:

$$\left| M_o V_o - \left(M + \sum_{i=1}^{\nu} (\mu \cdot_i + \sigma \cdot_i) + \sum_{j=1}^{2N} (H_j + G_j) \right) V \right| / M_o V_o \le \epsilon_1 \quad (53)$$

where ϵ_1 is the error tolerance. In this manner, errors in the overall mass balance may be used to ascertain whether the time step of integration should be decreased or the number of lumped groups increased.

The second criterion was based on the premise that accurate lumping must yield equivalent values for the total growing homopolymer concentration (Eq. 24) and the sum of the concentrations for the lumped growing homopolymer concentrations (Eqs. 43-45). Therefore, a comparison of these values was used to determine the accuracy of the lumping technique:

$$\left| \frac{M \cdot}{\sum_{i=1}^{\nu} \mu \cdot_i} - 1 \right| \le \epsilon_2 \quad (54)$$

In the final criterion, the concentration of the maximum chain length group, was evaluated to ensure that the maximum chain length, N, was large enough such that the resulting concentration of the maximum chain length group was negligible.

Kinetic rate coefficients

In the CPMWD formulation, the concentration- or chain-length-dependent reaction rate coefficients for homopolymerization can easily be handled, as previously demonstrated by the simulations of gel effect in the polymerization of polymethylmethacrylate (Chaimberg and Cohen, 1990). For the case of graft polymerization, the surface reactions involving the growing graft polymer species may be hindered due to the presence of a graft polymer layer. In particular, the polymer grafting reaction, in which a growing chain in solution reacts with a surface site, may be severely retarded due to steric hindrance effects imposed by adjacent grafted polymer chains. The effects of steric hindrance may be more pronounced for porous substrates, where the size of the polymer limits its diffusion into the porous infrastructure.

In a study that demonstrates the effect of steric hindrance on grafting, Papirer and Nguyen (1973) determined the influence of the polymer molecular weight on the graft yield for the reaction of a live homopolymer chain and an active surface site. The graft yield was shown to be independent of polymer molecular weight for grafting experiments at low polymer concentration. Conversely, at high polymer concentrations the graft yield was inversely related to the polymer molecular weight. The decrease in the surface coverage with increasing molecular weight of the graft polymer is primarily a result of steric hindrance effects in which a grafted polymer chain can shield adjacent reactive sites from the reactive polymer species in solution. In addition, large polymer chains in solution require a larger unobstructed area for grafting to occur.

The chain-length- and graft-polymer-concentration-dependent kinetic rate coefficients for the graft polymerization reaction were developed empirically following the formulation proposed by Tulig and Tirrell (1981). Based on the self-diffusion coefficient, derived from the reptation model of de Gennes (1971), the kinetic rate coefficient for polymer grafting, $k_{pMS(n,G)}$, of a growing homopolymer species with chain length n, $M \cdot_n$, and a surface site, S, at a grafted polymer concentration equal to G, is taken to be of the form:

$$k_{pMS(n,G)} = k_{pMS\cdot} \quad G \le G_c \quad (55)$$

$$k_{pMS(n,G)} = k_{pMS\cdot} \left(\frac{G_c}{G} \right)^{\beta} \left(\frac{1+N_c}{n+N_c} \right)^2 \quad G \ge G_c \quad (56)$$

where G_c is the critical graft polymer concentration at which the rate coefficient changes from being chain-length- and graft-polymer-concentration-independent ($k_{pMS\cdot}$) to becoming chain-length- and graft-polymer-concentration-dependent. The critical chain length, N_c, determines the length at which the rate coefficient begins to approach $1/n^2$ behavior (Coyle et al., 1985). The value of β was determined to be 1.75 based on extensive evaluation of experimental data (Chaimberg, 1989). The above form of the dependence of the reaction rate coefficients on chain length and the graft yield was also assumed to hold for the termination of grafted chains, via reactions 15 and 16, and for graft polymerization (Eq. 6).

To incorporate the chain length dependency of the reaction rate coefficients into the CPMWD model, one must derive the lumped rate coefficients for the lumped groups. For example, the rate of combination termination, $r_{tcMS(a,b)}$, of a group of growing homopolymers with chain lengths a_1 through a_n reacting with a group of growing grafted polymers with chain lengths b_1 through b_n is given by:

$$r_{tcMS}(a,b) = \sum_{i=a_1}^{a_n} \sum_{j=b_1}^{b_n} k_{tcMS(i,j)} M \cdot_i S \cdot_j \quad (57)$$

Lumping of the individual combination termination rate coef-

ficients over the range of the chain lengths for the a and b groups leads to the following approximation (Chaimberg and Cohen, 1990):

$$r_{tcMS}(a,b) \approx \bar{r}_{tcMS}(a,b) = \kappa_{tcMS(a,b)} \sum_{i=a_1}^{a_n} \sum_{j=b_1}^{b_n} M_{\cdot i} S_{\cdot j} \quad (58)$$

where $\bar{r}_{tcMS(a,b)}$ is the lumped rate of combination termination and $\kappa_{tcMS(a,b)}$ is the lumped rate coefficient for combination termination of lumped groups a and b. Consequently, by lumping the growing homopolymer and grafted polymer chains into groups the following form of the rate of combination termination is derived:

$$\bar{r}_{tcMS}(a,b) = \kappa_{tcMS(a,b)} \mu_{\cdot a} \sigma_{\cdot b} \quad (59)$$

Three different methods were evaluated for calculating the lumped combination termination rate coefficients: mean chain length, integral mean value and summation mean value. In the mean chain length method, the rate coefficients are determined using the mean chain length of the two lumped groups:

$$\kappa_{tcMS(a,b)} = k_{tcMS}\left(\frac{a_1+a_n}{2}, \frac{b_1+b_n}{2}\right) \quad (60)$$

The integral mean value termination rate coefficients, determined by integration of the individual termination rate coefficients over the two lumped groups, are given as:

$$\kappa_{tcMS(a,b)} = \frac{1}{(a_n-a_1)} \frac{1}{(b_n-b_1)} \int_{b_1}^{b_n} \int_{a_1}^{a_n} k_{tcMS(i,j)} di dj \quad (61)$$

Finally, the summation mean value termination rate coefficients, derived by summation of the individual termination rate coefficients over the two lumped groups, are given as:

$$\kappa_{tcMS(a,b)} = \frac{1}{(a_n-a_1+1)} \frac{1}{(b_n-b_1+1)} \sum_{i=b_1}^{b_n} \sum_{j=a_1}^{a_n} k_{tcMS(i,j)} \quad (62)$$

It has been previously demonstrated (Chaimberg and Cohen, 1990) that the model predictions for monomer conversion and polymer average molecular weight based upon the three different lumped termination rate coefficients (Eqs. 60-62) were within *a deviation of 0.005%* from each other. Thus, the small relative error introduced by the lumped kinetic rate coefficients of the above lumping technique is acceptable given the significant reduction in the number of equations to be solved.

Results and Discussion

The application of the CPMWD algorithm was illustrated for the free-radical graft polymerization of vinylpyrrolidone onto vinyl-modified silica. The graft polymerization reaction system, consisting of an aqueous suspension initiated with hydrogen peroxide and ammonium hydroxide, has been described in detail in previous publications (Chaimberg et al., 1989; Chaimberg and Cohen, 1991). The reaction rate parameters for vinylpyrrolidone graft polymerization used in this study were obtained, in part, from the kinetic model developed by Woodhams (1954) to describe the free-radical homopolymerization of vinylpyrrolidone (VP) in aqueous solution initiated with hydrogen peroxide and ammonia (Fikentscher and Herrle, 1945). According to the early studies on VP polymerization, PVP formation is enhanced by the ability of ammonium ions to catalyze the formation of hydrogen peroxide radicals. In addition, the alkalinity produced by the ammonium ions prevents the acid decomposition of vinylpyrrolidone into pyrrolidone and acetaldehyde (Woodhams, 1954; Breitenbach, 1957), and creates the optimal pH range for the polymerization reaction (Kwei, 1963). The overall dependence of the rate of homopolymerization, r_p, on the monomer concentration was shown to have the following form:

$$r_p = K_p \left(\frac{fK_d[I]}{K_t}\right)^{0.5} [M] \quad (63)$$

in which the initiation efficiency was found to be a function of the monomer concentration (Woodham, 1954).

$$f = \frac{K_{iM}}{K_d}(NH_4^+)(M) \quad (64)$$

Thus, from Eqs. 63 and 64 it is apparent that $r_p \propto (M)^{3/2}$. A number of investigators (see Hunkeler, 1991; and references therein) have suggested initiation mechanisms that can account for the 1.5 order of the rate of polymerization reaction. Other investigators (Woodhams, 1954; Billmeyer, 1984; Biesenberger and Sebastian, 1983) have proposed that one can rationalize the 1.5 order of reaction by viewing the initiation efficiency as being proportional to the monomer concentration. It is important to note that from the viewpoint of the CPMWD algorithm, when the order of the reaction does not change with monomer concentration, both approaches lead to an equivalent set of kinetic equations since the various initiation parameters are lumped.

Kinetic rate parameters for homopolymerization of vinylpyrrolidone

The reaction and kinetic rate parameters used in the graft polymerization reaction simulations for vinylpyrrolidone are shown in Table 1. The kinetic rate coefficients for homopolymer propagation, k_{pMM}, and homopolymer termination, $k_{tcMM} + k_{tdMM}$, were determined experimentally by Agasandyan et al. (1966) for free-radical bulk polymerization using azo-

Table 1. Reaction and Kinetic Rate Parameters for Vinylpyrrolidone Graft Polymerization

	Ref.
$\rho_M = 1.0488\{1 - 0.00086\,[T(\mathrm{K}) - 293.15]\}$, g/mL	*
$\rho_H = \rho_M/\{1 - 0.103\,\rho_M\}$, g/mL	*
$k_{pMM} = 1.122 \times 10^{+10} \exp[-7.10(\mathrm{kcal/mol})/\mathrm{RT}]$, L/(mol·min)	*
$k_{tcMM} + k_{tdMM} = 6.00 \times 10^{+10} \exp[-1.60(\mathrm{kcal/mol})/\mathrm{RT}]$, L/(mol·min)	*
$k_d = 4.30 \times 10^{+15} \exp[-30.2(\mathrm{kcal/mol})/\mathrm{RT}]$, min^{-1}	**
$f_M = 0.05$ [M]	**
$k_{trMM} = 5.61 \times 10^{+7} \exp[-7.10(\mathrm{kcal/mol})/\mathrm{RT}]$, L/(mol·min)	**
$k_{trMX} = 0$	†

* Agasandyan et al. (1966)
** Chaimberg (1989)
† Karaputadze et al. (1978)

Table 2. CPMWD Model Parameters for Vinylpyrrolidone Graft Polymerization Simulations

Lumped Group	Lump Size	First Chain	Last Chain
1-9	1	1	9
10-14	2	10	19
15-30	5	20	99
31-120	10	100	999
121-320	20	1,000	4,999
321	1	5,000	5,000

bisisobutyronitrile (AIBN) as the initiator. The rate of hydrogen peroxide decomposition is a function of the ammonium ion concentration (Woodhams, 1954), the pH of the reaction solution (Galbács and Csányi, 1983), and is known to be extremely sensitive to heterogeneous decomposition resulting from trace amounts of impurities and reaction vessel walls (Woodhams, 1954; Galbács and Csányi, 1983; Evans and Upton, 1985). Literature kinetic data were not reported for the rate of initiation using hydrogen peroxide and ammonium hydroxide. Therefore, the values of the rate coefficient of initiator decomposition, k_d, and the initiator efficiency, f_M, were estimated by comparing the predicted monomer conversion with the experimental data (Chaimberg and Cohen, 1991), and by requiring that the overall activation energy for the vinylpyrrolidone homopolymerization reaction be equal to 21.4 kcal/mol (Woodhams, 1954). The observed dependence of the rate of homopolymerization on the monomer concentration, that is, $r_p \propto (M)^{3/2}$, was incorporated into the current model by setting the initiator efficiency to be proportional to the monomer concentration (Eq. 64), analogous to polymerization reactions performed at high conversion and low efficiency (Biesenberger and Sebastian, 1983; Billmeyer, 1984). Other approaches that utilize a modified initiation mechanism *may* be possible, as was discussed by Hunkeler (1991) for the persulfate-initiated polymerization of *polyacrylamide*. However, as was discussed earlier, in the application of the CPMWD algorithm for the PVP/silica system *both* approaches lead to equivalent lumped kinetic parameter sets. No literature value was available for the kinetic rate coefficient for chain transfer to monomer, although molecular weight data obtained from PVP homopolymerization studies suggests that chain transfer to monomer may be significant (Breitenbach, 1957; Woodhams, 1954; Senogles and Thomas, 1978). Previous studies have demonstrated that chain transfer reactions with water (Karaputadze et al., 1978), ammonia (Woodhams, 1954), and hydrogen peroxide (Shtamm et al., 1981) are negligible for the range of initiator concentrations used in this study. Model simulations revealed, as expected, that chain transfer to monomer dominated the prediction of the average molecular weight. The value of k_{trMM} was estimated to be $0.005 \times k_{pMM}$ by fitting the model to the experimental conversion data, and the kinetic rate coefficients for combination and disproportionation termination were found to be nearly identical. Given the scatter in the reported data these rate constants were taken to be equal.

Graft polymerization sensitivity analysis

Reaction rate constants for vinylpyrrolidone polymerization reactions involving surface-grafted species have not been reported in the literature. To first illustrate the effect of the various surface grafting reactions, exploratory CPMWD model simulations were carried out using the model parameters shown in Table 2. In the first illustration, the kinetic rate parameters for the grafting reactions were taken to be equivalent to those of the homopolymer reaction (that is, $k_{pMM} = k_{pMS} = k_{pSM}$). Also, unless otherwise indicated the reaction rate coefficients for the graft polymerization termination reactions were taken to equal the homopolymerization termination (that is, $k_{tdMS} = k_{tdMM}$, $k_{tcMS} = k_{tcMM}$). The effect of varying the kinetic rate coefficients upon the predicted values of the conversion, graft yield and homopolymer and graft polymer average molecular weight for a representative reaction system ($M_o = 2.81$ mol/L, $T = 70°C$) is illustrated in the results of Table 3. Due to the negligible surface site concentration (Table 1) compared to that of the monomer in the *PVP/silica system* (for example, initial ratio $S_o/M_o < 0.001$), the monomer was consumed primarily via the formation of homopolymer. Consequently, incorporating the surface grafting reactions did not significantly affect the predicted values of the monomer conversion or homopolymer average molecular weight obtained from the homopolymeri-

Table 3. Sensitivity of Kinetic Rate Parameters on Conversion, Graft Yield, and Polymer Molecular-Weight Averages for $M_o = 2.81$ mol/L, $T = 70°C$, Reaction Time = 500 min

Kinetic Rate Parameters	Conversion	Graft Yield (mg/m^2)	Homopolymer M_w	Homopolymer M_n	Graft Polymer M_w	Graft Polymer M_n
BASIS*	0.883	2,775.39	42,500	21,300	64,700	42,800
$k_{pMS} = 0.1 \times k_{pMM}$	0.883	611.71	43,900	22,000	65,200	43,100
$k_{pMS} = 0.01 \times k_{pMM}$	0.883	68.90	44,200	22,100	65,300	42,900
$k_{pMS} = 0$	0.883	0.83	44,200	22,200	43,900	21,900
$k_{pMS} = 0$; $k_{tcMS} = 0$; $k_{tdMS} = 0$	0.883	0.87	44,200	22,200	45,600	22,700
$k_{pMS} = 0$; $k_{tcSS} = 0$; $k_{tdSS} = 0$	0.883	0.83	44,200	22,200	43,900	21,900
$k_{pSM} = 0$	0.883	1,337.18	42,500	21,300	42,500	21,200
$k_{pSM} = 0$; $k_{tcMS} = 0$; $k_{tdMS} = 0$	0.883	1,391.02	42,500	21,300	42,300	21,100
$k_{pSM} = 0$; $k_{tcSS} = 0$; $k_{tdSS} = 0$	0.883	1,377.40	42,500	21,300	42,500	21,200
$k_{tcMS} = 0$; $k_{tdMS} = 0$	0.883	2,825.87	42,500	21,300	65,200	43,100
$k_{tcSS} = 0$; $k_{tdSS} = 0$	0.883	2,777.96	42,500	21,300	64,700	42,800

* $k_d = 4.3 \times 10^{+15} \exp[-30.2(\text{kcal/mol})/RT]$ min^{-1}
$f_M = 0.05$ (M); $f_S = 0.05$ (S)
$k_{pMM} = k_{pMM} = k_{pMM} = 1.122 \times 10^{+10} \exp[-7.10(\text{kcal/mol})/RT]$ L/(mol·min)
$k_{trMM} = k_{trMS} = 5.61 \times 10^{+7} \exp[-7.10(\text{kcal/mol})/RT]$ L/(mol·min)
$k_{tcMM} = k_{tdMM} = k_{tcMS} = k_{tdMS} = k_{tcSS} = k_{tdSS} = 3.00 \times 10^{+10} \exp[-1.60(\text{kcal/mol})/RT]$ L/(mol·min)

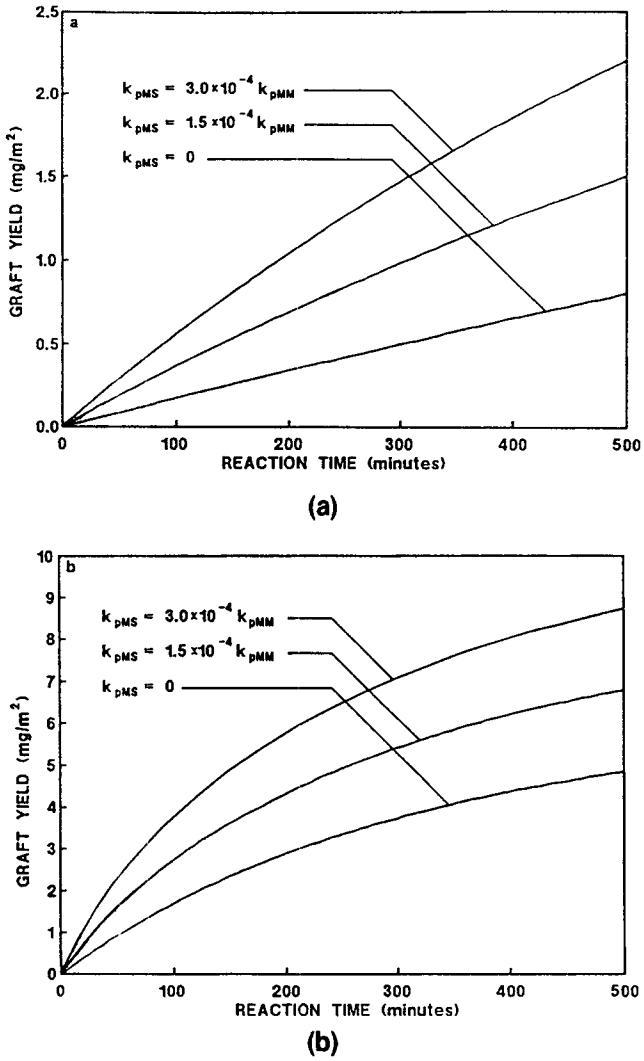

Figure 3. CPMWD-predicted PVP graft yield using different values of the polymer grafting rate coefficient for: a. $M_o = 0.936$ mol/L, $T = 70°C$; b. $M_o = 2.81$ mol/L, $T = 90°C$.

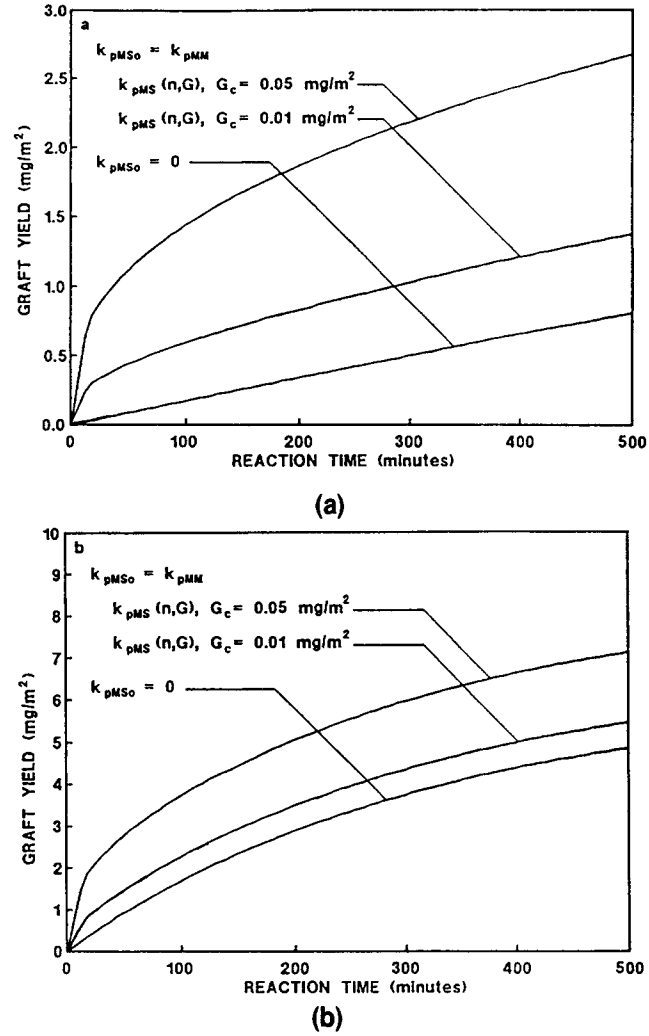

Figure 4. CPMWD-predicted PVP graft yield using different values of the graft-yield- and chain-length-dependent polymer grafting rate coefficient for: a. $M_o = 0.936$ mol/L, $T = 70°C$; b. $M_o = 2.81$ mol/L, $T = 90°C$.

zation reaction simulations. For the surface-grafted polymer, the results of the sensitivity analysis demonstrate that graft yield was more sensitive to the rate of polymer grafting than the rate of graft polymerization (Eq. 6). This result can be explained by the fact that polymer grafting of a single growing polymer chain composed of n monomer units (Eq. 5) results in a larger mass of grafted polymer than does the graft polymerization of a single monomer unit (Eq. 6). Thus, in contrast to the predicted graft yield values, the predicted average molecular weight of the surface-grafted polymer was influenced by both the polymer grafting and the graft polymerization reactions. Simulations were also conducted with values of the rate coefficients for grafted polymer-grafted polymer termination (k_{tcSS}, k_{tdSS}) ranging from either zero to the upper limit being the value of the homopolymer termination rate constants (see Table 3). These simulations suggest that the dependence of the graft yield and molecular weight of the surface-grafted polymer on the rate of termination of grafted chains via grafted polymer-grafted polymer termination is negligible. The above results are not surprising since, in the PVP/silica reaction system of Chaimberg and Cohen (1991), the concentration of growing grafted chains *was significantly lower* than the concentrations of monomer and growing homopolymer chains.

Polymer grafting, graft polymerization and chain transfer reactions were found to have a pronounced effect on the graft yield. In order to illustrate the coupled effect of these reactions, a series of numerical simulations were performed for varying values of the kinetic rate coefficients for the polymer grafting, graft polymerization and chain transfer reactions. As an illustration, two sets of reaction conditions from Chaimberg and Cohen (1991) which produced distinctly different experimental graft yield values are discussed: (a) $M_o = 0.936$ mol/L, $T = 70°C$; (b) $M_o = 2.81$ mol/L, $T = 90°C$. The predicted graft yields determined using different values of the kinetic rate coefficient for the polymer grafting reaction, k_{pMS}, are shown in Figures 3a and 3b. The model simulations reveal, as illustrated in Figures 3a and 3b, that the polymer grafting reaction can contribute significantly to the amount of surface-grafted polymer even when the polymer grafting rate constant is orders of magnitude smaller than the rate constant for ho-

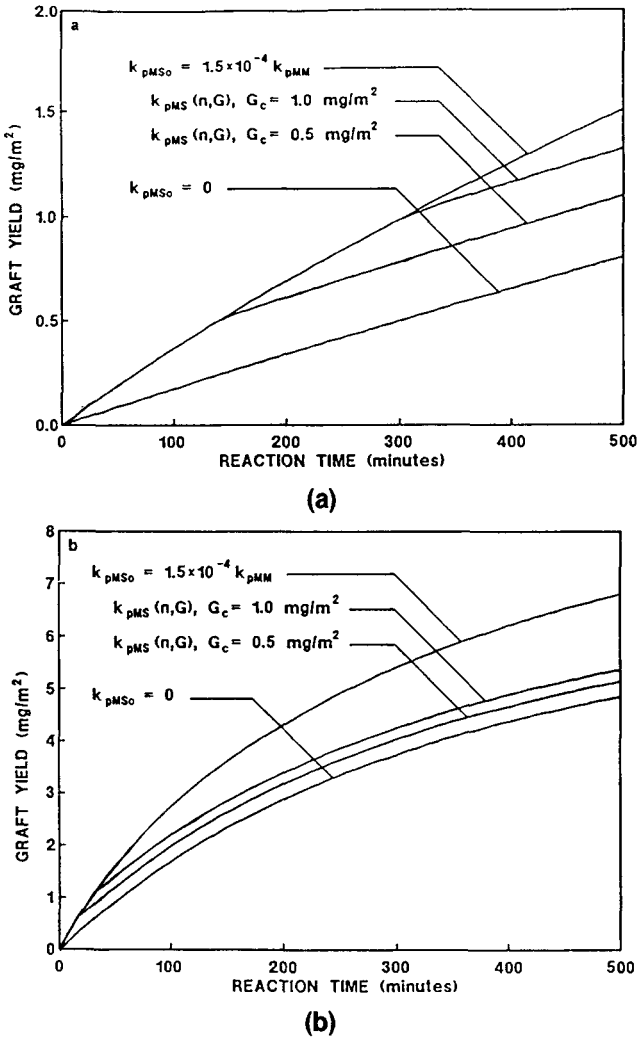

Figure 5. CPMWD-predicted PVP graft yield using different values of the graft-yield- and chain-length-dependent polymer grafting rate coefficient for: a. $M_o = 0.936$ mol/L, $T = 70°C$; b. $M_o = 2.81$ mol/L, $T = 90°C$.

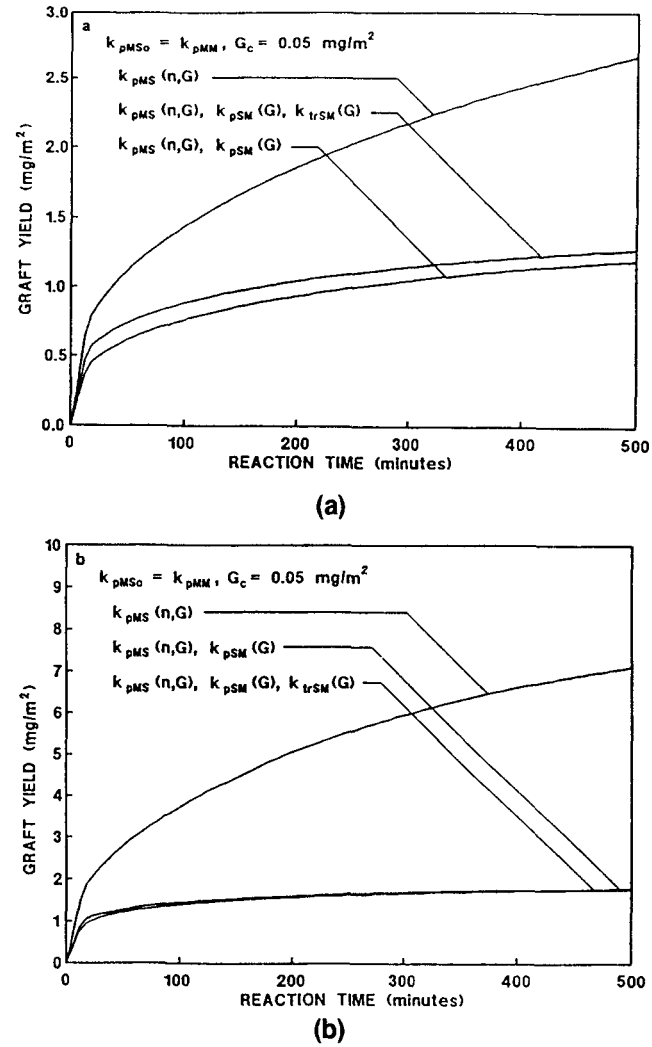

Figure 6. CPMWD-predicted PVP graft yield incorporating different values of the graft-yield- and chain-length-dependent polymer grafting rate coefficient, and the graft-yield-dependent graft polymerization and chain transfer to monomer rate coefficients for: a. $M_o = 0.936$ mol/L, $T = 70°C$; b. $M_o = 2.81$ mol/L, $T = 90°C$.

mopolymer propagation. It is important to note that these simulations do not show the plateau observed in the experimental graft yield data at large values of the reaction time. Thus, it is evident that the form of the kinetic rate coefficients must include a term which is linked to the graft polymerization reaction.

Better agreement with the experimental data is obtained when the effects of chain length and graft yield on the kinetic rate coefficients were included. For the polymer grafting reaction, a growing homopolymer chain reacts with a vinyl surface site. Due to the expected steric hindrance and diffusional resistance involved in the reaction of the growing homopolymer chain with a surface site (Eq. 5), the kinetic rate coefficient for the polymer grafting reaction, $k_{pMS}(n,G)$, was taken to be a function of the chain length of the growing homopolymer, n, and the graft polymer concentration, G (see Eqs. 55 and 56). Correspondingly, the reaction of the growing polymer chain with a surface site (Eq. 5) in the absence of any surface-grafted polymer may also be diffusion-limited, and thus, k_{pSMo} may be different than the rate constant, k_{pMM}. Comparisons of the CPMWD model predictions for the graft yield for two values of k_{pMSo} and two corresponding values of the critical graft polymer concentration, G_c, are shown in Figures 4 and 5. These model comparisons indicate that incorporation of the chain length and graft polymer concentration dependency for the rate of polymer grafting resulted in *lower* predicted values of the graft yield. However, as mentioned previously, the model did not predict the plateau region of the graft yield data at large values of the reaction time as reported by Chaimberg and Cohen (1991). Consequently, the significance of implementing graft-yield-dependent kinetic rate coefficients for the graft polymerization and chain transfer to monomer reactions of the growing graft polymer species, $k_{pSM}(G)$ and $k_{trSM}(G)$, was also examined. For the graft polymerization and chain transfer reactions, the reacting species in solution is a monomer and thus, the kinetic rate coefficients were taken to be solely dependent upon the concentration of grafted polymer. It is suggested that the decrease in the rates of these reactions with

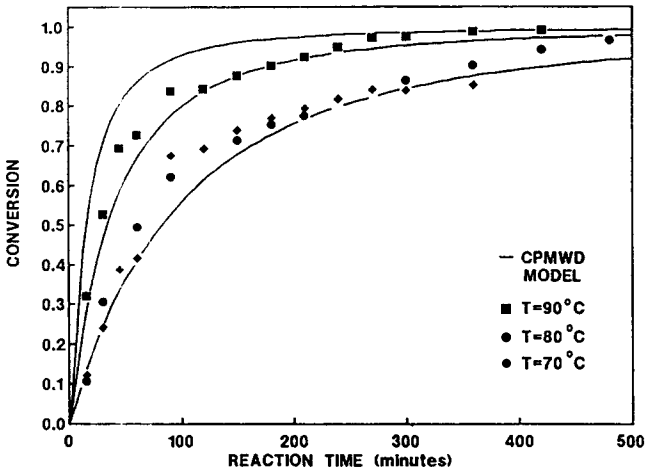

Figure 7. Experimental and CPMWD-predicted vinylpyrrolidone conversion for $M_o = 0.936$ mol/L (Chaimberg and Cohen, 1991).

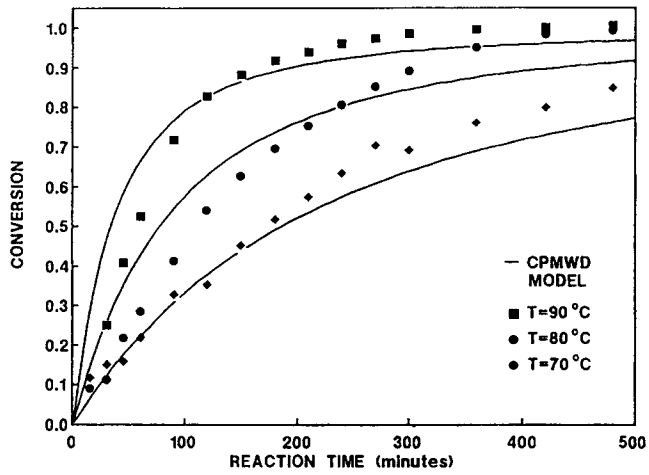

Figure 9. Experimental and CPMWD-predicted vinylpyrrolidone conversion for $M_o = 4.68$ mol/L (Chaimberg and Cohen, 1991).

increasing graft yield results from the increased diffusional resistance due to the surface-grafted polymer layer. As illustrated in Figures 6a and 6b, by incorporating a dependency of the rates of graft polymerization and chain transfer on graft yield, the CPMWD model predicted the plateau region of the graft yield. This suggests that once a prescribed amount of polymer has been grafted to the surface of the substrate (the critical graft polymer concentration), the rate of subsequent graft polymer formation was diminished.

Vinylpyrrolidone graft polymerization simulations

The complete CPMWD model incorporated the chain-length- and graft-polymer-concentration-dependent kinetic rate coefficient for polymer grafting, $k_{pMS}(n,G)$, and the graft-polymer concentration-dependent kinetic rate coefficients for graft polymerization, $k_{pSM}(G)$, and chain transfer, $k_{trMS}(G)$. Our parameter analysis using both the monomer conversion and graft yield data resulted in the best-fit parameter set in which $G_c = 0.5$ mg/m^2, $K_{pMSo} = 1.5 \times 10^{-4} k_{pMM}$ and where both k_{pSM} and k_{trMS} are dependent on chain length while k_{pMS} is a function of both chain length and the graft yield.

The CPMWD algorithm with the best-fit kinetic parameter values was used to study the free radical graft polymerization reaction of vinylpyrrolidone onto a vinyl-silane modified silica substrate for a temperature range of 70°C-90°C and an initial monomer concentration range of 0.936 mol/L to 4.68 mol/L. As shown in Figures 7 to 9, the CPMWD model reasonably predicted the monomer conversion for the prescribed set of initial monomer concentrations and reaction temperatures. As mentioned above, due to the relatively *low* concentration of the surface reactive sites as compared to the monomer concentration, the effect of variations in the rates of the grafting

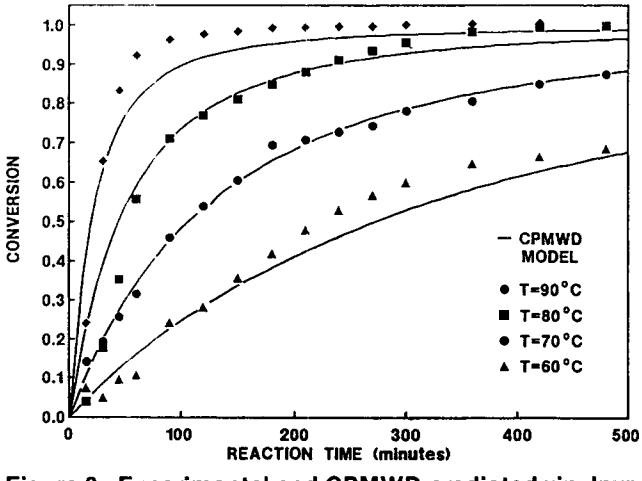

Figure 8. Experimental and CPMWD-predicted vinylpyrrolidone conversion for $M_o = 2.81$ mol/L (Chaimberg and Cohen, 1991).

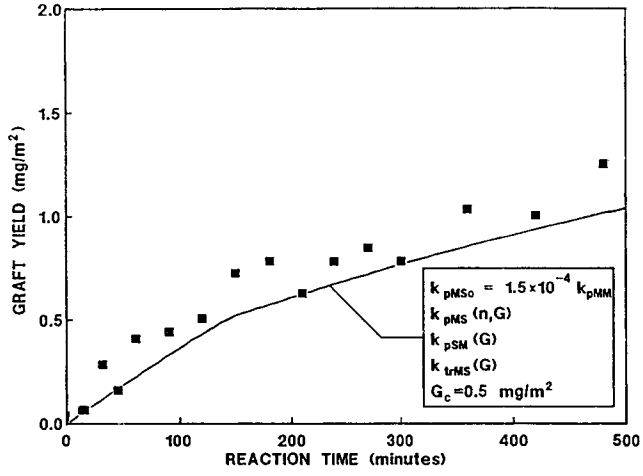

Figure 10. Experimental and CPMWD-predicted PVP graft yield using best-fit graft-yield- and chain-length-dependent polymer grafting rate coefficient, and the critical graft yield for $M_o = 0.936$ mol/L, $T = 70$°C (Chaimberg and Cohen, 1991).

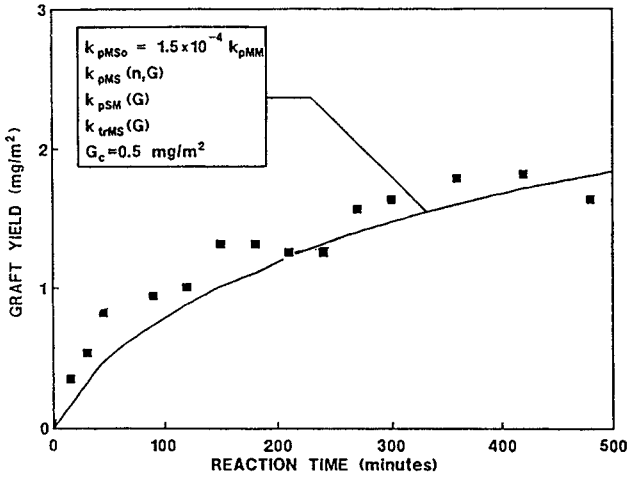

Figure 11. Experimental and CPMWD-predicted PVP graft yield using best-fit values of the graft-yield- and chain-length-dependent polymer grafting rate coefficient, and the critical graft yield for $M_o = 0.936$ mol/L, $T = 80°C$ (Chaimberg and Cohen, 1991).

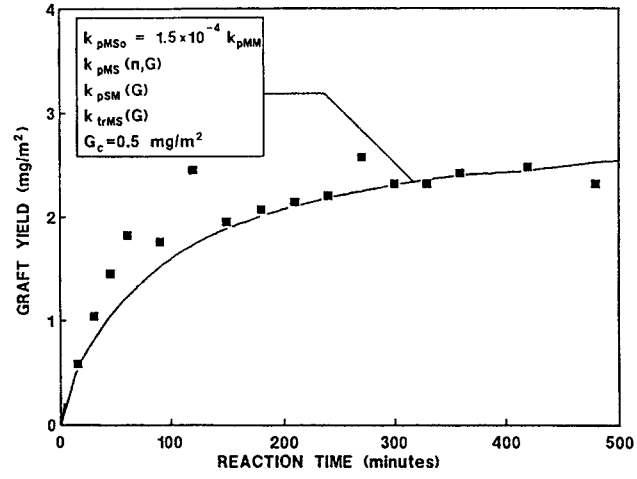

Figure 13. Experimental and CPMWD-predicted PVP graft yield using best-fit values of the graft-yield- and chain-length-dependent polymer grafting rate coefficient, and the critical graft yield for $M_o = 2.81$ mol/L, $T = 90°C$ (Chaimberg and Cohen, 1991).

reactions on monomer conversion was negligible. The CPMWD model predictions for the graft yield as a function of reaction time are shown in Figures 10 through 15 for several reaction conditions. In general, the trend in the graft yield data was predicted by the CPMWD model. Deviations from the experimental graft yield values were observed, however, for the case of the high initial monomer concentration ($M_o = 4.68$ mol/L), in which the values of the graft yield data continued to increase throughout the reaction while the numerical predictions tended to approach plateau values. The above behavior may be partially linked to the polymer grafting reaction which was found to significantly affect the graft yield. Although, in the CPMWD model, the kinetic rate coefficient for polymer grafting was taken to be a function of the grafted polymer concentration, it is plausible that the rate of graft polymer formation could also depend on the uniformity and MWD of the surface-grafted polymer layer. The latter effects were not considered due to the lack of data on the characteristics of the grafted polymer layer and further work in this direction is warranted.

MWD of homopolymer and graft polymer

The CPMWD model was used to predict the molecular weight distribution of both the homopolymer and surface-grafted polymer. From these distributions, it was possible to calculate the

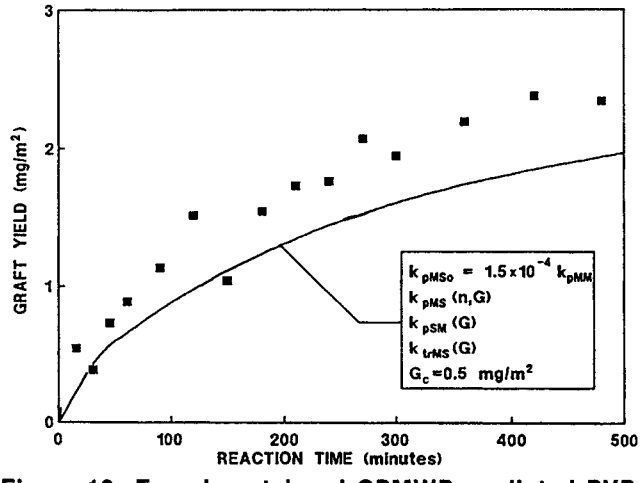

Figure 12. Experimental and CPMWD-predicted PVP graft yield using best-fit values of the graft-yield- and chain-length-dependent polymer grafting rate coefficient, and the critical graft yield for $M_o = 2.81$ mol/L, $T = 80°C$ (Chaimberg and Cohen, 1991).

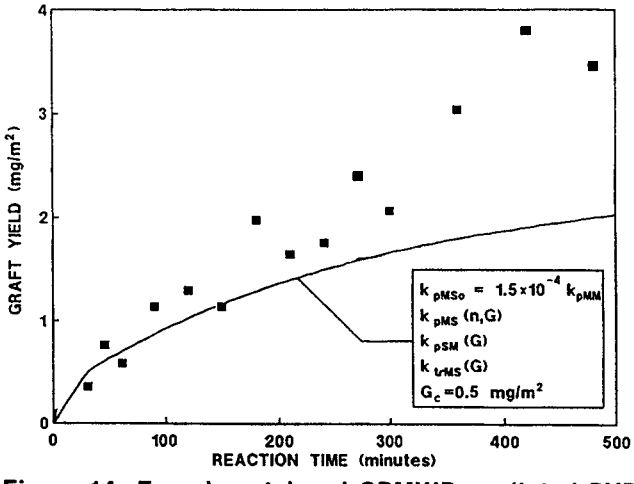

Figure 14. Experimental and CPMWD-predicted PVP graft yield using best-fit values of the graft-yield- and chain-length-dependent polymer grafting rate coefficient, and the critical graft yield for $M_o = 4.68$ mol/L, $T = 80°C$ (Chaimberg and Cohen, 1991).

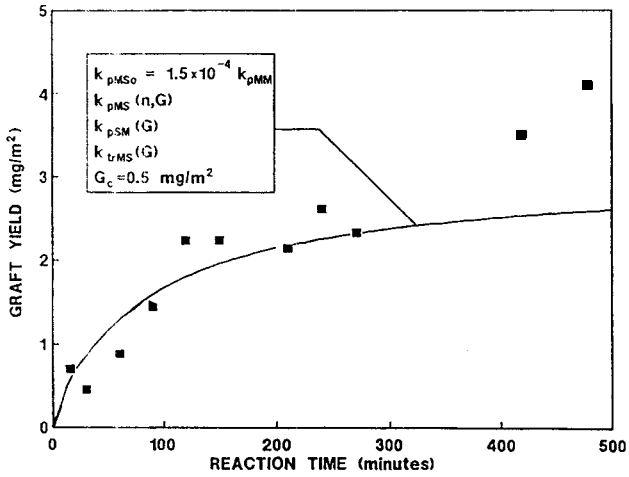

Figure 15. Experimental and CPMWD-predicted PVP graft yield using best-fit values of the graft-yield- and chain-length-dependent polymer grafting rate coefficient, and the critical graft yield for $M_o = 4.68$ mol/L, $T = 90°C$ (Chaimberg and Cohen, 1991).

number- and weight-average molecular weights (Table 4). For comparison, the homopolymer and graft polymer average molecular weight predictions for the case of invariant kinetic rate coefficients are included. A comparison of the predicted average molecular weights for the different kinetic rate parameters indicates that incorporation of the chain-length- and graft-polymer-concentration-dependent kinetic rate coefficients does not alter the homopolymer average molecular weight values but it does lower the predicted molecular weights of the graft polymer. Examination of the predicted values of molecular weights of the homopolymer for each set of reaction conditions indicate that while these values were within 5% of each other, there was a general trend of increasing average molecular weights for increasing initial monomer concentrations and decreasing reaction temperatures. It is important to note that there is an *uncertainty* regarding the estimate of the activation energy for the rate coefficient of chain transfer to monomer (the dominant reaction in the molecular weight determination), which was assumed to be equal to the activation energy for the homopolymer propagation. Furthermore, it is conceivable that chain transfer reactions to other species, such as initiator,

Table 4. Predicted Average Molecular Weight of Homopolymer and Surface-Grafted Polymer*

T (°C)	M_o (mol/L)	Homopolymer M_w	Homopolymer M_n	Graft Polymer M_w	Graft Polymer M_n
70	0.936	43,500	21,800	47,600	23,900
70	2.81	44,200	22,200	49,000	24,700
70	4.68	44,500	22,300	49,500	25,000
80	0.936	42,400	21,300	37,700	17,200
80	2.81	43,500	21,800	49,200	17,800
80	4.68	43,900	22,000	39,700	17,900
90	0.936	41,200	20,600	30,700	12,100
90	2.81	42,700	21,400	32,300	12,500
90	4.68	43,200	21,700	33,000	12,600

* $k_{pSMo} = 1.5 \times 10^{-4} k_{pMM}$; $G_c = 0.5$ mg/m²

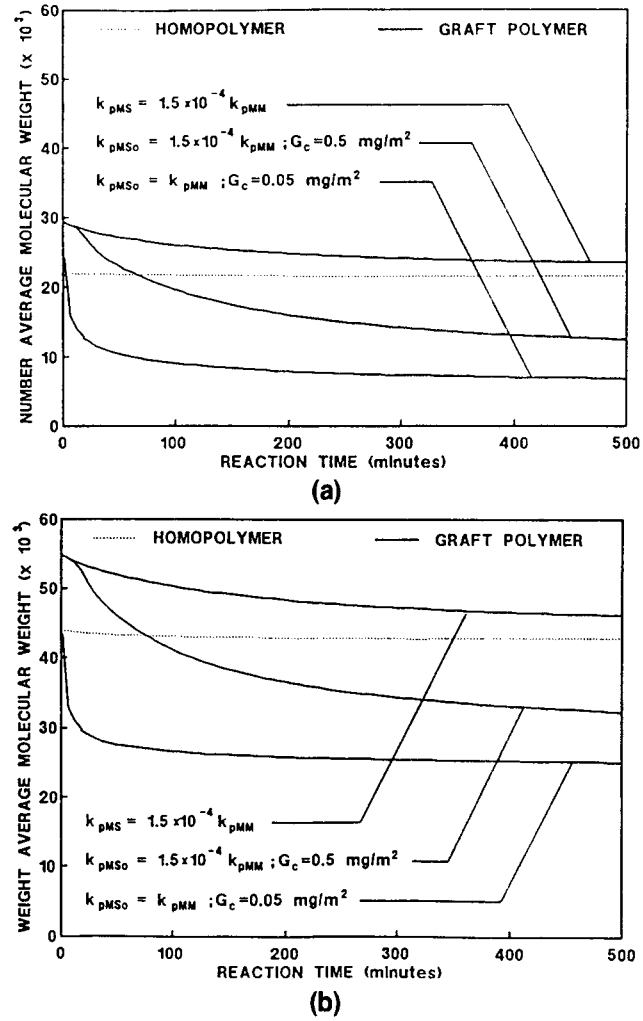

Figure 16. CPMWD model predictions of: a. number-average molecular weight vs. reaction time for $M_o = 2.81$ mol/L, $T = 80°C$; b. weight-average molecular weight vs. reaction time for $M_o = 2.81$ mol/L, $T = 80°C$.

co-catalyst, and so on, may prove to be important (Woodhams, 1954). Thus, the variation of the molecular weight with temperature as predicted for the PVP/silica system would be affected by the above uncertainties. Clearly, more detailed experimental studies are needed in order to accurately quantify the temperature variation of the kinetic rate coefficients for chain transfer, graft polymerization, polymer grafting and graft polymer termination.

In order to better illustrate the influence of the kinetic rate parameters on the molecular weight distribution of the polymer, the average molecular weight values as a function of reaction time are plotted for one representative reaction condition (see Figures 16a and 16b). These results demonstrate that the average molecular weights (M_w and M_n) of the surface polymer are significantly reduced when the rate of polymer grafting is hindered due to steric effects (see Eqs. 55 and 56). Also, it is noted that the polymer grafting reaction significantly affects the molecular weight of the resulting surface polymer even when the rate coefficient for graft polymerization (k_{pMS}) is assumed to be significantly lower than the rate coefficient for the graft polymer propagation rate coefficient.

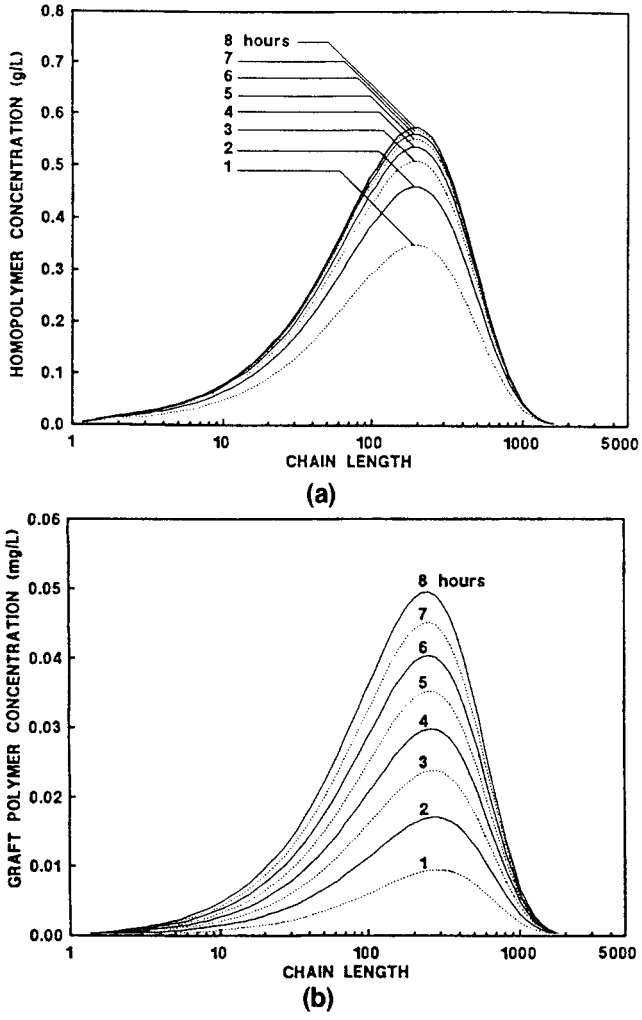

Figure 17. CPMWD model predictions, using invariant kinetic rate coefficients, of: a. homopolymer cumulative MWD vs. reaction time for M_o = 2.81 mol/L, T = 80°C; b. graft polymer cumulative MWD vs. reaction time for M_o = 2.81 mol/L, T = 80°C.

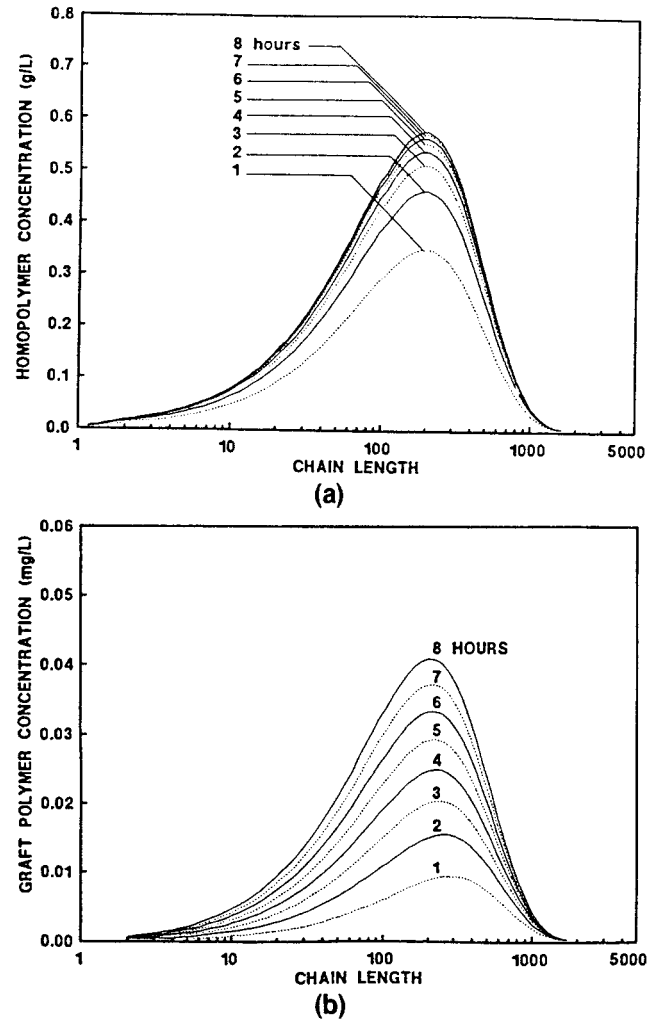

Figure 18. CPMWD model predictions, using chain-length- and graft-yield-dependent kinetic rate coefficients, of: a. homopolymer cumulative MWD vs. reaction time for M_o = 2.81 mol/L, T = 80°C; b. graft polymer cumulative MWD vs. reaction time for M_o = 2.81 mol/L, T = 80°C.

Finally, the cumulative molecular weight distributions for the homopolymer and graft polymer are illustrated in Figures 17 and 18 for the representative simulations at one set of reaction conditions using the invariant and variable kinetic rate coefficients, respectively. It is demonstrated that the homopolymer MWD is not affected by the rate of polymer grafting. The graft polymer MWD, however, is shifted to a lower distribution once the chain length and concentration dependence of the rate of polymer grafting is employed.

Summary and Conclusions

A CPMWD kinetic model, in which the rate coefficients may be chain-length- or concentration-dependent, was developed to study free-radical graft polymerization kinetics. The algorithm of the CPMWD model is based upon the use of an implicit numerical technique to solve for the coupled monomer, surface site, and total growing polymer concentration differential equations. Acceleration of the numerical calculations was achieved by lumping the growing polymer chains into distinct groups. The CPMWD method is not limited by the type of radical initiation or chain transfer reactions. Furthermore, the CPMWD model is ideally suited to graft polymerization reactions with low graft yield values since the CPMWD algorithm maintains an accurate mass balance.

The application of the CPMWD model was demonstrated for the free-radical graft polymerization of vinylpyrrolidone onto silica. It was shown that the CPMWD algorithm reasonably predicted the monomer conversion and graft yield for a wide range of reaction conditions. Improvements to the CPMWD predictions for the specific example of PVP/silica system may be achieved by independent experimental determinations of the kinetic rate coefficients for the free-radical graft polymerization reaction system. For example, as in the case of diffusion-controlled polymerization (Mita and Horie, 1987), the dependency of the kinetic rate coefficients on the chain length of the reacting species, or upon the solution properties, such as viscosity, may prove to be important. Furthermore, because the grafting reactions are heterogeneous

(involving two different phases) one must be aware of the possible complications due to adsorption, diffusion and steric hindrance effects. Finally, it is important to note that although the results of the present study with the CPMWD model is encouraging, one requires accurate MWD data, especially for the low molecular weight range of graft polymerized chains, for definitive quantitative evaluation of the CPMWD approach. A different challenge, however, is in degrafting the terminally anchored chains for the purpose of molecular weight analysis. Although, Chaimberg and Cohen (1991) have recently demonstrated an experimental technique for estimating the molecular weight of grafted PVP, via degrafting with hydrofluoric acid, sample purification problems with their method resulted in very approximate average molecular weight data. An additional complication is in obtaining accurate molecular weight distribution for the low molecular weight range expected for chains grafted via graft polymerization. In this regard, recent advances in size exclusion chromatography (SEC) in which a low angle laser light scattering (LALLS) detector is coupled with a concentration detector may provide the tool for developing the necessary accurate MWD data.

Acknowledgment

This work was funded in part by the National Science Foundation under Grant CBT-8416719, the National Science Foundation Engineering Research Center on Hazardous Substance Control under Grant CDR-22184, the United States Geological Survey Department of Interior under Award 14-08-0001-G1315 and the Water Resources Center (University of California) Project W-660.

Notation

f_M = initiator efficiency for monomer
f_S = initiator efficiency for surface sites
G = total dead grafted polymer concentration (graft yield)
G_c = critical dead grafted polymer concentration
G_i = dead grafted polymer species of chain length i, or its molar concentration
H_i = dead homopolymer species of chain length i, or its molar concentration
I = initiator species, or its molar concentration
I_o = initial molar concentration of initiator
k_d = rate coefficient for initiator decomposition
k_{iM} = rate coefficient for monomer initiation
k_{iS} = rate coefficient for surface site initiation
k_{pMM} = rate coefficient for homopolymer propagation
k_{pMS} = rate coefficient for polymer grafting
k_{pMSo} = rate coefficient for chain-length-independent polymer grafting
k_{pSM} = rate coefficient for graft polymer propagation
k_{pSMo} = rate coefficient for chain-length-independent graft polymer propagation
k_{tcMM} = rate coefficient for homopolymer-homopolymer combination termination
k_{tcMS} = rate coefficient for homopolymer-graft polymer combination termination
k_{tcSS} = rate coefficient for graft polymer-graft polymer combination termination
k_{tdMM} = rate coefficient for homopolymer-homopolymer disproportionation termination
k_{tdMS} = rate coefficient for homopolymer-graft polymer disproportionation termination
k_{tdSS} = rate coefficient for graft polymer-graft polymer disproportionation termination
k_{trMM} = rate coefficient for homopolymer-monomer chain transfer
k_{trMS} = rate coefficient for homopolymer-surface site chain transfer
k_{trMX} = rate coefficient for homopolymer-solvent chain transfer
k_{trSM} = rate coefficient for graft polymer-monomer chain transfer
k_{trSMo} = rate coefficient for chain-length-independent graft polymer-monomer chain transfer
k_{trSS} = rate coefficient for graft polymer-surface site chain transfer
k_{trSX} = rate coefficient for graft polymer-solvent chain transfer
M = monomer in solution, or its molar concentration
M_n = number average molecular weight
M_o = initial molar concentration of monomer
M_w = weight average molecular weight
$M\cdot$ = total growing polymer species, or its molar concentration
$M\cdot_i$ = growing polymer species of chain length i or its molar concentration
N = maximum chain length of a growing polymer
N_c = critical chain length parameter for chain-length-dependent rate coefficients
r_{tcMM} = rate of homopolymer-homopolymer combination termination
$\bar{r}_{tcMM}$ = rate of lumped homopolymer-homopolymer combination termination
R = universal gas constant
$R\cdot$ = initiator radical, or its molar concentration
S = surface reactive site, or its molar concentration
$S\cdot$ = total growing grafted polymer species, or its molar concentration
$S\cdot_i$ = growing grafted polymer species of chain length i, or its molar concentration
t = time
T = temperature
V = volume of reaction system
V_o = initial volume of reaction system
x = monomer conversion
X = solvent species, or its molar concentration

Greek letters

$\delta_{i,j}$ = parameter used in the lumping model
ϵ = fractional volume contraction
ϵ = error tolerance
κ_{pMM} = lumped rate coefficient for homopolymer propagation
κ_{pMS} = lumped rate coefficient for polymer grafting
κ_{pMSo} = lumped rate coefficient for chain-length-independent polymer grafting
κ_{pSM} = lumped rate coefficient for graft polymer propagation
κ_{tcMM} = lumped rate coefficient for homopolymer-homopolymer combination termination
κ_{tcMS} = lumped rate coefficient for homopolymer-graft polymer combination termination
κ_{tcSS} = lumped rate coefficient for graft polymer-graft polymer combination termination
κ_{tdMM} = lumped rate coefficient for homopolymer-homopolymer disproportionation termination
κ_{tdMS} = lumped rate coefficient for homopolymer-graft polymer disproportionation termination
κ_{tdSS} = lumped rate coefficient for graft polymer-graft polymer disproportionation termination
κ_{trMM} = lumped rate coefficient for homopolymer-monomer chain transfer
κ_{trMS} = lumped rate coefficient for homopolymer-surface site chain transfer
κ_{trMX} = lumped rate coefficient for homopolymer-solvent chain transfer
κ_{trSM} = lumped rate coefficient for graft polymer-monomer chain transfer
κ_{trSS} = lumped rate coefficient for graft polymer-surface site chain transfer
κ_{trSX} = lumped rate coefficient for graft polymer-solvent chain transfer
λ_j = number of chains in the jth group
$\mu\cdot_i$ = ith group of growing homopolymer chains used in the lumping model, or its molar concentration
ν = total number of lumped groups used in the lumping model
ρ_H = homopolymer density
ρ_M = monomer density
$\sigma\cdot_i$ = ith group of growing grafted polymer chains used in the lumping model, or its molar concentration
ϕ_{Mo} = initial volume fraction of monomer

Subscripts

$k_{(n)}$ = rate coefficient for reaction of polymer with chain length equal to n

$k_{(m,n)}$ = rate coefficient for reaction of polymers with chain lengths equal to m and n

Literature Cited

Agasandyan, V. A., E. A. Trosman, Kh. S. Bagdasar'yan, A. D. Litmanovich, and V. Ya. Shtern, "Determination of Absolute Rate Constants of Chain Propagation and Termination in the Polymerization of N-Vinylpyrrolidone," *Vysokomol. Soyed.*, **8**, 1580 (1966).

Biesenberger, J. A., and D. H. Sebastian, *Principles of Polymerization Engineering*, Wiley-Interscience, New York (1983).

Billmeyer, F. W., *Textbook of Polymer Science*, 3rd ed., Wiley-Interscience, New York (1984).

Breitenbach, J. W., "Polymerization and Polymers of N-Vinylpyrrolidone," *J. Polym. Sci.*, **23**, 949 (1957).

Browne, T., M. Chaimberg, and Y. Cohen, "Graft Polymerization of Vinyl Acetate onto Silica," *J. Appl. Polym. Sci.*, **44**, 671 (1992).

Chaimberg, M., "Free Radical Graft Polymerization of Vinylpyrrolidone," PhD Thesis, Univ. of California, Los Angeles (1989).

Chaimberg, M., R. Parnas, and Y. Cohen, "Graft Polymerization of Polyvinylpyrrolidone onto Silica," *J. Appl. Polym. Sci.*, **37**, 2921 (1989).

Chaimberg, M., and Y. Cohen, "Kinetic Modeling of Free-Radical Polymerization: A Conservation Polymerization and Molecular Weight Distribution Model," *Ind. Eng. Chem. Res.*, **29**, 1152 (1990).

Chaimberg, M., and Y. Cohen, "Free-Radical Graft Polymerization of Vinylpyrrolidone onto Silica," *Ind. Eng. Chem. Res.*, **30**, 2534 (1991).

Chiu, W. Y., G. M. Carratt, and D. S. Soong, "A Computer Model for the Gel Effect in Free-Radical Polymerization," *Macromolec.*, **16**, 348 (1983).

Cohen, Y., and P. Eisenberg, "Silica Polyvinylpyrrolidone-Grafted Resins: A Promising Packing Material for Size Exclusion Chromatography of Water Soluble Polymers," *Polyelectrolyte Gels: Properties, Preparation, and Applications*, R. S. Harland and R. K. Prud'homme, eds., ACS (1992).

Cohen, Y., P. Eisenberg, and M. Chaimberg, "Permeability of Graft Polymerized Polyvinylpyrrolidone-Silica Resin in Packed Columns," *J. Colloid Interface Sci.*, **148**, 579 (1992).

Coyle, D. J., T. J. Tulig, and M. Tirrell, "Finite Element Analysis of High Conversion Free-Radical Polymerization," *Ind. Eng. Chem. Fund.*, **24**, 343 (1985).

de Gennes, P. G., "Reptation of a Polymer Chain in the Presence of Fixed Obstacles," *J. Chem. Phys.*, **55**, 572 (1971).

Domb, A., and Y. Avny, "Graft Polymerization of Propylene Sulfide on Crosslinked Polystyrene," *J. Appl. Polym. Sci.*, **29**, 2517 (1984).

Edelson, D., "On the Solution of Differential Equations Arising in Chemical Kinetics," *J. Comput. Phys.*, **11**, 455 (1973).

Evans, D. F., and M. W. Upton, "Studies on Singlet Oxygen in Aqueous Solution. Part 4. The 'Spontaneous' and Catalyzed Decomposition of Hydrogen Peroxide," *J. Chem. Soc., Dalton Trans.*, 2525 (1985).

Fikentscher, H., and H. Herrle, "Polyvinylpyrrolidone," *Modern Plastics*, **11**, 157 (1945).

Fox, T. G., M. S. Gluckman, F. Gornick, R. K. Graham, and S. Gratch, "Graft Copolymers from Polymers Having Pendent Mercaptan Groups: I. Kinetic Considerations," *J. Polym. Sci.*, **37**, 397 (1959).

Galbács, Z. M., and L. J. Csányi, "Alkali-induced Decomposition of Hydrogen Peroxide," *J. Chem. Soc., Dalton Trans.*, 2353 (1983).

Gear, W. C., *Numerical Initial Value Problems in Ordinary Differential Equations*, Prentice-Hall, Englewood Cliffs, NJ (1971).

Gelinas, R. J., "Stiff Systems of Kinetic Equations. Practitioner's View," *J. Comput. Phys.*, **9**, 222 (1972).

Heffernan, J. G., and D. C. Sherrington, "Polystyrene Gel Permeation Chromatography Packings Grafted with Polar Monomers—Synthesis and Use in Aqueous Organic Mobile Phases," *J. Appl. Polym. Sci.*, **29**, 3013 (1984).

Hernandez, J., "Kinetic Studies of High Impact Polystyrene," MS Thesis, McMaster Univ., Hamilton, Ontario, Canada (1990).

Hunkeler, D., "Mechanism and Kinetics of the Persulfate-Initiated Polymerization of Acrylamide," *Macromolec.*, **24**, 2160 (1991).

Ito, K., "Derivation of Distribution of the Degree of Polymerization by Probability Theory," *J. Polym. Sci. A-2*, **7**, 241 (1969).

Karaputadze, T. M., V. I. Shumskii, and Yu. E. Kirsh, "Effect of the Type of Solvent on Radical Polymerization of N-Vinylpyrrolidone," *Vysokomol. Soyed.*, **A20**, 1854 (1978).

Korshak, V. V., L. B. Zubakova, N. V. Kachurina, and O. B. Balashova, "Chemical Grafting of Vinyl Heterocyclic Monomers to the Surface of Mineral Carriers," *Vysokomol. Soyed.*, **A21**, 2 (1979).

Krasilnikov, I., and V. Borisova, "Adsorption and Chromatographic Properties of Modified Silica Sorbents for the Production of Viral Preparations," *J. Chromatogr.*, **446**, 211 (1988).

Kwei, K. S., "The Influence of pH on the Polymerization of VP," *Polym. Lett.*, **1**, 379 (1963).

Laible, R., and K. Hamann, "Formation of Chemically Bound Polymer Layers on Oxide Surfaces and Their Role in Colloidal Stability," *Adv. Colloid Interf. Sci.*, **13**, 65 (1980).

Mita, I., and K. Horie, "Diffusion-Controlled Reactions in Polymer Systems," *J. Macromol. Sci.-Rev. Macromol. Chem. Phys.*, **C27**, 91 (1987).

Monrabal, B., "Polystyrene Bonded Silica as GPC Packing: A Variable Pore Diameter Packing Concept in GPC," *Liquid Chromatography of Polymers and Related Materials: III*, J. Crazes, ed., Chromatog. Sci. Ser. 19, Marcel Dekker, New York, p. 79 (1981).

Nayak, P. L., S. Lenka, and N. C. Pati, "Grafting Vinyl Monomers onto Wool Fibers: I. Graft Copolymerization of Methyl Methacrylate onto Wool Using V^{5+}-Thiourea Redox System," *J. Appl. Polym. Sci.*, **22**, 3301 (1978).

Papirer, E., and V. T. Nguyen, "Étude Cinétique du Greffage de Polystyrène Anionique sur les Silices: Contraction des Macromolécules sur la Surface Solide," *Angew. Makromol. Chem.*, **28**, 31 (1973).

Parnas, R. S., M. Chaimberg, V. Taepaisitphongse, and Y. Cohen, "The Adsorption of Polyvinylpyrrolidone and Polyethylene Oxide onto Chemically Modified Silica," *J. Colloid Interf. Sci.*, **129**, 441 (1989).

Raval, D. K., R. G. Patel, and V. S. Patel, "Grafting of Methyl Methacrylate onto Guar Gum by Hydrogen Peroxide Initiation," *J. Appl. Polym. Sci.*, **35**, 2201 (1988).

Sahoo, P. K., H. S. Samantaray, and R. K. Samal, "Graft Copolymerization with New Class of Acidic Peroxo Salts as Initiators: I. Grafting of Acrylamide onto Cotton-Cellulose Using Potassium Monopersulfate, Catalyzed by Co(II)," *J. Appl. Polym. Sci.*, **32**, 5693 (1986).

Samal, R. K., S. C. Satrusallya, and P. K. Sahoo, "Hexavalent-Chromium-Initiated Graft Copolymerization of Methyl Methacrylate onto Cellulose," *J. Appl. Polym. Sci.*, **29**, 319 (1984).

Samal, S., G. Sahu, and P. L. Nayak, "Grafting Vinyl Monomers onto Silk Fibers: Graft Copolymerization of Methyl Methacrylate onto Silk Using Acetylacetonate Mn(III) Complex," *J. Appl. Polym. Sci.*, **29**, 3283 (1984).

Senogles, E., and R. Thomas, "Polymerization Kinetics of *N*-Vinylpyrrolidone," *J. Polym. Sci. Symp.*, **49**, 203 (1975).

Senogles, E., and R. A. Thomas, "Hydrogen Bonding Effects in the Polymerization of *N*-Vinylpyrrolidone," *J. Polym. Sci., Polym. Lett. Ed.*, **16**, 555 (1978).

Shtamm, E. V., T. M. Karaputadze, Yu. E. Kirsh, A. P. Purmal', and Yu. I. Skurlatov, "Mechanism of the Polymerization of *N*-Vinylpyrrolidone in the Photolytic Decomposition of Hydrogen Peroxide," *Zhur. Fiz. Khim.*, **55**, 2289 (1981).

Skeirik, R. D., and E. A. Grulke, "A Calculation Scheme for Rigorous Treatment of Free Radical Polymerization," *Chem. Eng. Sci.*, **40**, 535 (1985).

Sundardi, F., "Graft Copolymerization of Hydrophilic Monomers onto Irradiated Polypropylene Fibers," *J. Appl. Polym. Sci.*, **22**, 3163 (1978).

Tripathy, S. S., S. Jena, S. B. Misra, N. P. Padhi, and B. C. Singh, "A Study of Graft Copolymerization of Methyl Methacrylate onto Jute Fiber," *J. Appl. Polym. Sci.*, **30**, 1399 (1985).

Tulig, T. J., and M. Tirrell, "Toward a Molecular Theory of the Trommsdorff Effect," *Macromolec.*, **14**, 1501 (1981).

Vasantha, R., K. P. Rao, and K. T. Joseph, "Synthesis and Characterization of Vegetable Tannin-Vinyl Graft Copolymers: I. Cutch-Poly(Methyl Acrylate) Graft Copolymers," *J. Appl. Polym. Sci.*, **33**, 2271 (1987).

Wheals, B. B., "Chemically Bonded Phases for Liquid Chromatography," *J. Chromatogr.*, **107**, 402 (1975).
Woodhams, R. T., *The Kinetics of Polymerization of Vinyl Pyrrolidone*, Polytechnic Univ., New York (1954).
Yablokova, N. V., Yu. A. Aleksandrov, and O. M. Titova, "Styrene Polymerization on Mineral Filler Surfaces, Modified with Organosilicon Peroxides," *Vysokomol. Soyed.*, **A28**, 1908 (1986).
Zubakova, L. B., V. N. Borisova, S. K. Koroleva, V. Ya. Davydov, and G. N. Filatova, "Study of the Chemistry of the Surface of an Adsorbent Based on Silokhrom and *N*-Vinylpyrrolidone," *Zh. Prik. Khim.*, **60**, 1491 (1987).

Manuscript received May 8, 1992, and revision received June 14, 1993.